ResearchGate

See discussions, stats, and author profiles for this publication at: https://www.researchgate.net/publication/272355404

Uzel-et-al-İzmir-Balikesir FZ and Menderes Exhumation EPSL

Data · February 2015

CITATIONS
0

READS
191

5 authors, including:

Cor Langereis
Utrecht University
208 PUBLICATIONS **6,975** CITATIONS
SEE PROFILE

Nuretdin KAYMAKCI
Middle East Technical University
101 PUBLICATIONS **1,567** CITATIONS
SEE PROFILE

Hasan Sozbilir
Dokuz Eylul University
125 PUBLICATIONS **2,152** CITATIONS
SEE PROFILE

Caglar Özkaymak
Afyon Kocatepe University
51 PUBLICATIONS **345** CITATIONS
SEE PROFILE

Some of the authors of this publication are also working on these related projects:

Project
Geology and Neotectonics of Alaşehir District View project

Project
Geodynamic relationship between the İzmir-Balıkesir Transfer Zone and the North Anatolian Fault Zone View project

All content following this page was uploaded by Nuretdin KAYMAKCI on 17 February 2015.

The user has requested enhancement of the downloaded file.

Earth and Planetary Science Letters 414 (2015) 108–125

Contents lists available at ScienceDirect

Earth and Planetary Science Letters

www.elsevier.com/locate/epsl

Paleomagnetic evidence for an inverse rotation history of Western Anatolia during the exhumation of Menderes core complex

Bora Uzel [a,*], Cornelis G. Langereis [b], Nuretdin Kaymakci [c], Hasan Sözbilir [a], Çağlar Özkaymak [d], Murat Özkaptan [c]

[a] Dokuz Eylül University, Department of Geological Engineering, TR-35160 İzmir, Turkey
[b] Utrecht University, Fort Hoofddijk Paleomagnetic Laboratory, 3584-CD Utrecht, The Netherlands
[c] Middle East Technical University, Department of Geological Engineering, TR-06531 Ankara, Turkey
[d] Afyon Kocatepe University, Department of Geological Engineering, TR-03200 Afyon, Turkey

ARTICLE INFO

Article history:
Received 22 August 2014
Received in revised form 3 January 2015
Accepted 6 January 2015
Available online 28 January 2015
Editor: A. Yin

Keywords:
Miocene
paleomagnetism
İzmir-Balıkesir Transfer Zone
Menderes metamorphic core complex
rotation
western Anatolia

ABSTRACT

Within the Aegean extensional system, the İzmir-Balıkesir Transfer Zone (İBTZ) is a crucial element in the late Cenozoic evolution of western Anatolia since it accommodates the differential deformation between the Cycladic and the Menderes metamorphic core complexes. Here, we determine the rotational history of western Anatolia using new paleomagnetic data from 87 sites in Miocene volcano-sedimentary rocks to better understand the role of the İBTZ. Our results reveal two discrete and opposite major rotational phases during the Miocene. The first phase is derived from early Miocene volcanic, sedimentary and granitic rocks and is controlled by detachment and strike-slip faults. It is characterized by an average (net) $23 \pm 6^\circ$ clockwise (CW) rotation within the İBTZ since the early Miocene. Our new data from the Menderes part on the other hand show an average $-23 \pm 10^\circ$ counter-clockwise (CCW) rotation. The data from the Cycladic part show no significant (net) rotation since the early Miocene. The second phase is derived from middle–late Miocene volcanic and sedimentary rocks and is controlled by high-angle normal and strike-slip faults. The rotations from this phase show a very consistent pattern of $-22 \pm 11^\circ$ CCW within the İBTZ, while now the Menderes part shows an average CW rotation of $25 \pm 14^\circ$.
Our paleomagnetic results hence document a major change and inversion of rotation. Between the early and late Miocene the İBTZ region experienced a large 45° CW rotation, while during the same time interval the Menderes part outside the zone experienced a similar (48°) CCW rotation. After that, the İBTZ became narrower and the sense of rotation inverted to CCW ($-23 \pm 10^\circ$ since the late Miocene), while in the Menderes part it inverted to CW ($25 \pm 14^\circ$ since the late Miocene). Our new results do therefore fit the hypotheses of two-stage-extension scenario, rather than a one-single-phase of extension. We also conclude that the observed rotations are not directly related to major detachment faulting, but to the change in extensional regime of western Anatolia. The focal mechanism solutions of recent seismic events corroborate that the İBTZ is still active and transfers west Anatolian extensional strain into the south Aegean Sea.

© 2015 Elsevier B.V. All rights reserved.

1. Introduction

The Western Anatolia is dominated by extension in the convergent setting of the Africa–Europe collision. This setting has resulted in core complex formation during ongoing subduction related slab edge processes along the Hellenic and Cyprean trenches (Wortel and Spakman, 2000; van Hinsbergen et al., 2010; Biryol et al., 2011) that gave way to the exhumation of large metamorphic core complexes (Hetzel et al., 1995, 2013; Emre and Sözbilir, 1997; Lips et al., 2001; Bozkurt and Oberhänsli, 2001; Sözbilir, 2001, 2002; Ring et al., 2003; Bozkurt and Sözbilir, 2004; Candan et al., 2001; Gessner et al., 2013). A vast amount of literature has accumulated on the geology and exhumation of the Menderes metamorphic core complex (MCC) in Western Anatolia and on the related kinematics of extensional deformation in the region (Fig. 1). Two end member models have been proposed for the Aegean—west Anatolian extension. One end member blames the westwards escape of Anatolia while the other invokes slab edge processes related to the northward subducting African slab below Eurasia (Le Pichon and Angelier, 1979; Meulenkamp et al., 1988;

* Corresponding author. Fax: +90 2324127300.
E-mail address: bora.uzel@deu.edu.tr (B. Uzel).

http://dx.doi.org/10.1016/j.epsl.2015.01.008
0012-821X/© 2015 Elsevier B.V. All rights reserved.

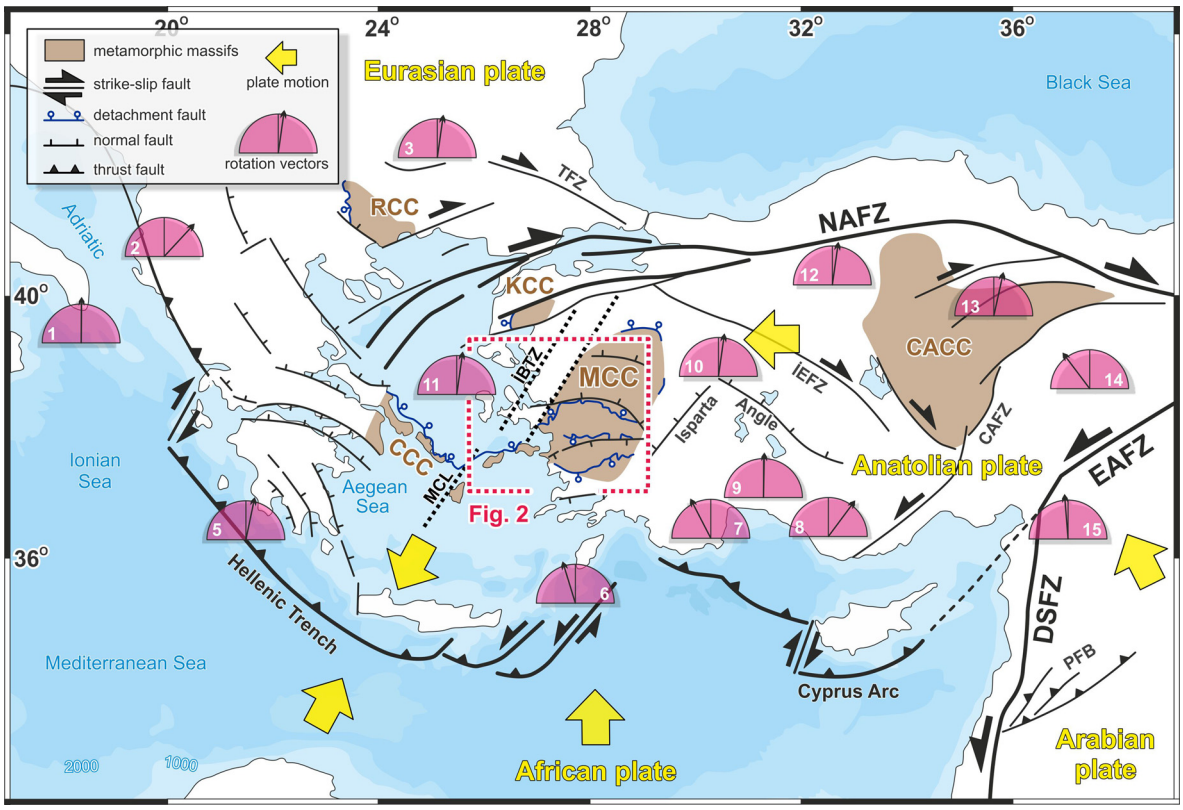

Fig. 1. Published paleomagnetic results from the eastern Mediterranean region. The map is compiled from Şengör et al. (1985), Barka (1992), Walcott and White (1998), Bozkurt (2001), Brun and Sokoutis (2007), Uzel et al. (2013), van Hinsbergen et al. (2010), Biryol et al. (2011) and our own observations. Pink half circles represent reliable paleomagnetic declinations for post-Eocene: 1) Apulian platform (Scheepers, 1992; Speranza and Kissel, 1993; van Hinsbergen et al., 2014), 2) Albania (Speranza et al., 1992, 1995; Mauritsch et al., 1995, 1996), 3) Moesian platform and Rhodope (van Hinsbergen et al., 2008), 4) western Greece and Peloponnesus (Horner and Freeman, 1982, 1983; Kissel et al., 1984, 1985; Kissel and Laj, 1988; Márton et al., 1990; Morris, 1995; van Hinsbergen et al., 2005b), 5) Crete (Duermeijer et al., 1998), 6) Rhodos (Laj et al., 1982; van Hinsbergen et al., 2007), 7) Bey Dağları (Kissel and Poisson, 1987; Morris and Robertson, 1993; van Hinsbergen et al., 2010b), 8) eastern limb of the Isparta Angle (Kissel et al., 1993), 9) center of the Isparta Angle (Kissel and Poisson, 1986), 10) Afyon (Gürsoy et al., 2003), 11) Lesbos (Kissel et al., 1989; Beck et al., 2001), 12) Galatean province (Krijgsman et al., 1996; Gürsoy et al., 1999), 13) Çiçekdağı basin (Gülyüz et al., 2013), 14) Sivas basin (Krijgsman et al., 1996; Platzman et al., 1998; Gürsoy et al., 1997), 15) NW margin of the Arabian platform (Gaziantep, Kilis) (Gürsoy et al., 2009). NAFZ, North Anatolian Fault Zone; EAFZ, East Anatolian Fault Zone; DSFZ, Dead Sea Fault Zone, PFB, Palmyride Fold Belt; CAFZ, Central Anatolian Fault Zone; İEFZ, İnönü–Eskişehir Fault Zone; TFZ, Thrace Fault Zone; İBTZ, İzmir-Balıkesir Transfer Zone; MCL, Mid-Cycladic Lineament. MCC, Menderes Metamorphic Core Complex; CCC, Cycladic Metamorphic Core Complex; KCC, Kazdağ Metamorphic Core Complex; RCC, Rhodope Metamorphic Core Complex; CACC, Central Anatolian Crystalline Complex.

van Hinsbergen et al., 2005a, 2010; Biryol et al., 2011). Naturally, there are many other models that include a combination of these two end members (for details see Bozkurt, 2001). Recent developments in tomography (van Hinsbergen et al., 2005a, 2010; Faccenna et al., 2003, 2006, 2013; Biryol et al., 2011; Gans et al., 2009) suggest that slab edge processes and related back-arc extension are the dominant driving force for the Western Anatolian and Aegean tectonics (Jolivet et al., 2013). According to this scenario, back arc extension in the region is compensated by large-scale extensional detachments and high-angle normal faults, along which a series of core complexes and gneissic domes are exhumed; it seems that each core complex accommodated a different amount of extension. Therefore, lateral variation of extension must be compensated by the development of accommodation zones or transfer faults. In Western Anatolia, the İzmir-Balıkesir Transfer Zone (İBTZ) is one of the major accommodation zones, first described by Sözbilir et al. (2003). Subsequently, field-based studies documented the stratigraphic and structural features of the İBTZ (Sözbilir et al., 2011; Uzel et al., 2013 and references therein). Recently, Gessner et al. (2013) suggested that the İBTZ is a surface expression of a tear in the subducting African Slab, *aka* the West Anatolian Shear Zone.

The İBTZ is a NE–SW trending strike-slip dominated shear zone that—to the east—marks the western termination of E–W striking grabens, while—to the west—it is linked to discrete loci of extension (Figs. 1 and 2) (Ring et al., 1999; Uzel and Sözbilir, 2008; Sözbilir et al., 2011; Uzel et al., 2013). To the southwest of the İBTZ, a similar major NE–SW-trending right-lateral strike-slip dominated zone exists: the Mid Cycladic Lineament (Walcott and White, 1998). This shear zone has been interpreted as the boundary between the eastern and western Aegean extensional domains (Morris and Anderson, 1996; Pe-Piper et al., 2002; Philippon et al., 2012). The İBTZ and Mid Cycladic Lineament together accommodate differential extensional strain between the CCC in the west and the MCC in the east.

Here, we aim at a better understanding of the kinematics of the İBTZ and consequently the regime of Western Anatolian extension by using paleomagnetism as a tool to detect vertical axis rotations in space and time. In due time, the results will be combined with ages from both available (published) radiometric age data and with new Ar^{40}/Ar^{39} data now being acquired (Uzel et al., in preparation).

A number of paleomagnetic studies have been carried out in western Anatolia, following the pioneering work of Kissel et al. (1987). Subsequently, many paleomagnetic studies have contributed to the paleomagnetic database of Western Anatolia and have provided constraints on vertical axis rotations in the region (Orbay et al., 2000; van Hinsbergen et al., 2010, 2010c, 2010a; Kondopoulou et al., 2011; Piper et al., 2010). Other paleomagnetic studies in the region were aimed at magnetostratigraphic dating of Neogene deposits (e.g. Şen and Seyitoğlu, 2009) or at regional tectonics (e.g. Kaymakci et al., 2007). But although there

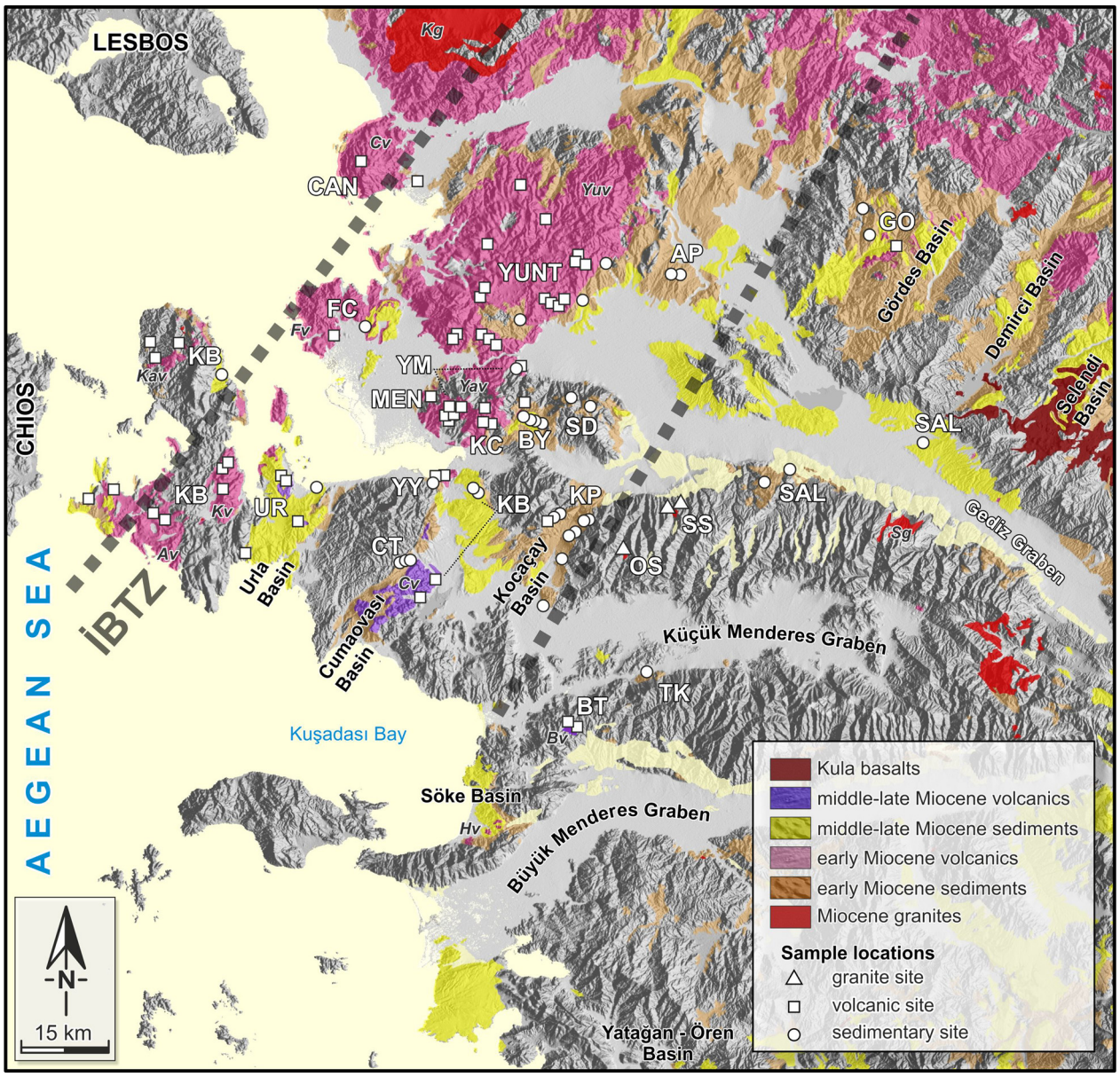

Fig. 2. Simplified geological map of western Anatolia (MTA, 2002) draped onto a Digital Elevation Model image showing the distribution of paleomagnetic sampling locations and their abbreviations (used throughout text and tables) in white. İBTZ, İzmir-Balıkesir Transfer Zone; Kg, Kozak granite; Sg, Salihli granite; Tg, Turgutlu granite; Kav, Karaburun volcanic suite, Kv, Kocadağ volcanic suite; Av, Armağandağ volcanic suite; Yuv, Yuntdağ volcanic suite; Yav, Yamanlar volcanic suite; Fv, Foça volcanic suite; Cv, Çandarlı volcanic suite; Hv, Hisartepe volcanics; Bv, Balatçık volcanics.

is already a large paleomagnetic database, most studies have addressed mainland Greece and the Aegean Islands, but too few have addressed—in sufficient detail—the tectonic history of the İBTZ and the Western Anatolian extensional regime.

2. Methods

2.1. Sampling strategy

Essentially, there are two strategies of sampling for paleomagnetic purposes: in extrusive volcanics or in sediments. Extrusive volcanic rocks accurately record the field as a 'spot reading' while sediments sloppily acquire the field over a longer time interval. The drawbacks and advantages of each strategy are well known, but pose practical problems if one wants to combine both volcanic and sediment data. Sampling strategy is constrained by the availability of suitable rock types. But perhaps more importantly, the most crucial source of error in determining vertical axes rotations (e.g. in Western Anatolia) is recognizing the size of the tectonic blocks. Bearing this in mind, we have sampled almost all volcanic and sedimentary units in the study area. Depending on the availability of (magmatic) material, each sampled site is, or will be, dated using the Ar^{40}/Ar^{39} radiometric technique (Uzel et al., in preparation); otherwise published age data are utilized.

In total, 1199 cores for paleomagnetic purposes were sampled at 87 localities. The drilling locations are concentrated on Miocene (volcano-stratigraphic or sedimentary) outcrops exposed along the İBTZ as well as in E–W and NE–SW striking basins (Fig. 2). Additionally, two syn-extensional granite bodies that intruded into the Menderes metamorphic core complex during its exhumation have been sampled. For each locality we grouped sites into logical (geologically coherent) clusters from which we determined the vertical axis rotations per block. To avoid any type of local deformation both around the volcanic centers and close to fault zones, we tar-

geted undeformed and fresh outcrops wherever possible. For more detailed information of the sampling sites, see Appendix 1 in supplementary data.

Samples were collected by drilling cores using a gasoline-powered drill. Sample orientations were always measured with a magnetic compass, but for volcanic rocks a sun compass was also used. The core orientations as well as the bedding tilts were corrected for the present-day declination (typically 4°W for the entire sampling period). We aimed at taking at least 12 (and up to as much as a hundred) standard oriented paleomagnetic cores at each site or section, in sediments usually after removing the weathered surface. Reversal and fold tests are applied if possible. In the course of this study, a number of locations were re-sampled because of the adverse effects of lightning, or because of low intensity values in the previously collected samples. Typically, a single core provides multiple specimens that could be used for both thermal (TH) and alternating field (AF) demagnetization experiments.

2.2. Paleomagnetic measurements

Samples were demagnetized using both alternating field (AF) and thermal (TH) progressive stepwise demagnetization methods. The thermal demagnetization was carried out in a magnetically shielded oven (ASC TD48-SC), with steps varying from 10–50 °C, up to a maximum of 645 °C. The AF demagnetization was carried out with increments of 3–20 mT, up to a maximum of 80 or 100 mT. The natural remanent magnetization (NRM) of all samples was measured on a 2G Enterprises horizontal 2G DC SQUID cryogenic magnetometer (noise level 3×10^{-12} Am^2). For AF demagnetization, an in-house developed robot assisted and fully automated 2G DC SQUID cryogenic magnetometer was used.

Thermomagnetic runs to determine magnetic carriers were carried out in air, using a modified horizontal translation type Curie balance, with a sensitivity of $\sim 5 \times 10^{-9}$ Am^2 (Mullender et al., 1993). Approximately 30–65 mg of powdered rock sample was put into a quartz-glass sample holder and was held in place by quartz wool. Heating and cooling rates were 10 °C/min. Temperatures were increased in a number of heating and cooling cycles up to a maximum of 700 °C. The anisotropy of magnetic susceptibility (AMS) was measured to determine the magnetic fabric of the sediments and to assess whether they have a mainly sedimentary or tectonic fabric (Hrouda, 1982). During deformation, the maximum axis of the AMS tensor (k_{max}) will gradually align with the direction of maximum extension and become perpendicular to the direction of maximum compression. For calculations of the susceptibility tensor, Jelinek statistics (Jelinek, 1978, 1981) were used.

Demagnetization diagrams of the NRM were analyzed from orthogonal vector diagrams (Zijderveld, 1967). We determined the characteristic remanent magnetization (ChRM) directions, by taking generally five to eight successive temperature or AF steps, using an eigenvector approach (Kirschvink, 1980). In several cases, samples with a direction that could not be entirely resolved due to a (partial) overprint were analyzed using the great-circle approach (of McFadden and McElhinny, 1988). Because the distribution of paleomagnetic directions induced by secular variation of the Earth's magnetic field is circular at the poles, but gradually becomes more ellipsoid towards the equator (e.g. Tauxe and Kent, 2004), we calculate site-means and virtual geomagnetic pole (VGP) distribution statistics (K, A95) and the corresponding errors in declination (ΔD_x) and inclination (ΔI_x) according to Butler (1992). Successively, we used a fixed cut-off (45°) and we follow Deenen et al. (2011, 2014) in assessing whether a VGP distribution can be ascribed to paleosecular variation through their N-dependent reliability envelope. To determine whether two distributions have a common true mean direction (ctmd), we used the reversal test developed by McFadden and McElhinny (1990) and their classifications (A, B, C, indeterminate). The classifications are based on the critical angle γ_c and the angle γ between the means. Because we use their test with simulation, the test is equivalent to using the V_w statistical parameter of Watson (1983).

The common temperature steps using thermal (TH) and alternating field (AF) demagnetization techniques are as follows; the volcanic sites were analyzed using progressive stepwise thermal demagnetization in typically 15 steps up to 630°, while the sedimentary rocks are analyzed in a maximum of 19 steps up to 610°. For the volcanics, we used 16 alternating field demagnetization steps up to 100 mT, while for the sedimentary specimens we used an additional 2 steps.

3. Paleomagnetic results

In many samples a small viscous component is removed at low temperatures (100–120 °C) or at low alternating fields (0–15 mT). Occasionally, a secondary present-day field component is present, and is generally removed at temperatures around 200–230 °C (Fig. 3). Demagnetization analysis supports that in many cases the principal magnetic carrier of the ChRM in the volcanics samples is (Ti-poor) magnetite, evidenced by maximum unblocking temperatures of 530–580 °C and alternating magnetic fields of 60–90 mT (Fig. 4). However, in the sediment samples, we find both magnetite unblocking temperatures and lower unblocking temperatures around 320–350 °C which could point to the presence a magnetic iron-sulfide like greigite which is quite common in sediments (e.g. Vasiliev et al., 2008). In most cases, thermomagnetic curves obtained by Curie Balance measurements (Fig. 4a–f) confirm the results of the thermal demagnetization. In volcanic samples the Curie temperature is mostly in the range 530–580 °C confirming (Ti-poor) magnetite as a carrier. The results of Anisotropy of Magnetic Susceptibility (AMS) measurements for some of sedimentary sites presenting in Fig. 4, shows well-clustered oblate and prolate shapes. In general, however, it needs further concern for an accurate-correlation between AMS results and tectonic directions/rotations, here we would only suggest that alignment of the maximum axis in magnetic fabrics are mostly parallel to the structural trend in the sampled area/basin (Figs. 2 and 4g) rather than aligned by the direction of water currents.

The sampled sites can be divided into two main tectonic domains: (i) the areas within the İBTZ and (ii) those outside of it (Fig. 2). Within the İBTZ we include nine areas: (1) Çandarlı, (2) Cumaovası, (3) Foça, (4) Karaburun East, (5) Kocaçay, (6) Spil, (7) Urla, (8) Yamanlar, and (9) Yuntdağ. Three localities are located outside of the İBTZ, which are: (1) Gördes, (2) Karaburun West and (3) the Grabens including the E–W-trending Gediz, Küçük Menderes, and Büyük Menderes grabens. The paleomagnetic analyses were firstly done on a per site basis, and then the site data were combined for each subarea and analyzed to obtain mean directions for the whole subarea.

3.1. Paleomagnetic results within the İBTZ

We have averaged the sites per locality where each locality forms a coherent, logical geological/tectonic block. In case we have only 2 sites per block, we have taken the average of all samples from the sites, provided the sites had the same rock type (only sediments or only volcanics), and only if the A95 values fall within the A95 confidence envelope of Deenen et al. (2011, 2014), implying that the distributions represent paleosecular variation. If we have 3 or more sites per block/locality, we took the mean of the sites as the locality mean, also to avoid complications in mixing results from different rock types. Indeed, in a number of cases—and always in volcanic sites—A95 was smaller than $A95_{min}$ signifying a spot reading of the field (indicated in Appendix 2); PSV is then

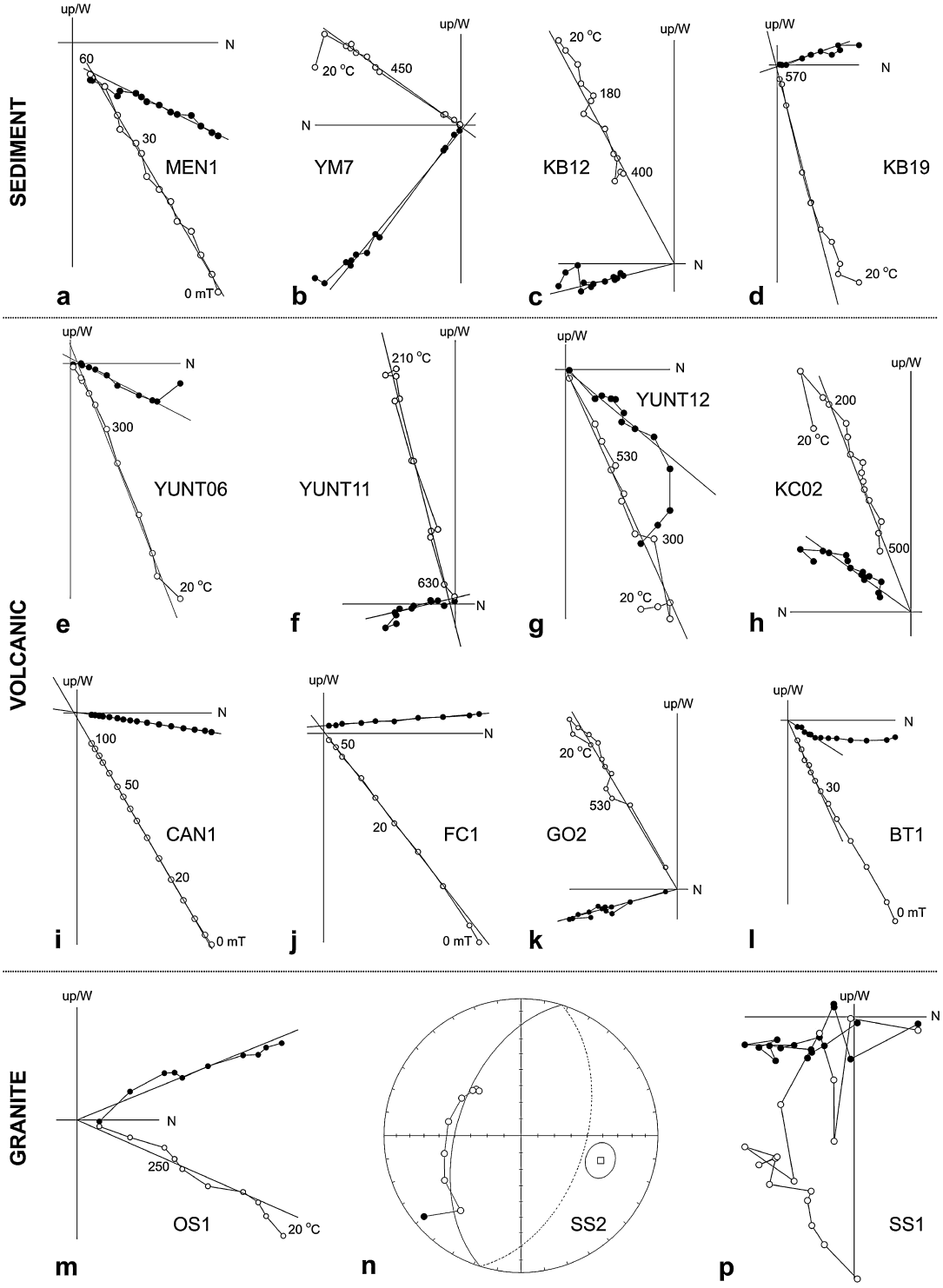

Fig. 3. Orthogonal vector diagrams (Zijderveld, 1967), showing characteristic demagnetization diagrams for representative samples from sedimentary, volcanic and granitic rocks. Closed (open) circles indicate the projection on the horizontal (vertical) plane. Alternating field (°C) and thermal (mT) demagnetization steps are indicated. All diagrams are in a tilt corrected reference frame. For some sites we calculated mean directions by including great circle solutions according to the method of McFadden and McElhinny (1988).

not averaged out. In describing the rotations, we use the declination with respect to North and its error (ΔD_x), and these results are plotted for each locality/block in Fig. 5. In Table 1 we summarize the results per block/locality and per age. Full results at the site level are reported in the Supplementary Information as Appendix 2.

Two early Miocene sites of Çandarlı area show coherent directions with a small uncertainty (Appendix 2). The individual site results are clustered in the NE quadrant. Taken together, these results show that the Çandarlı area underwent a clockwise (CW) vertical-axis rotation of $21 \pm 5°$, since the emplacement of the early Miocene volcanics (Figs. 5 and 6, Table 1).

The rotation results for the early Miocene (CT1–3, YY1–3) from the Cumaovası basin are rather consistent with dominantly reversed polairity. One site (CT03) shows both polarities with a pos-

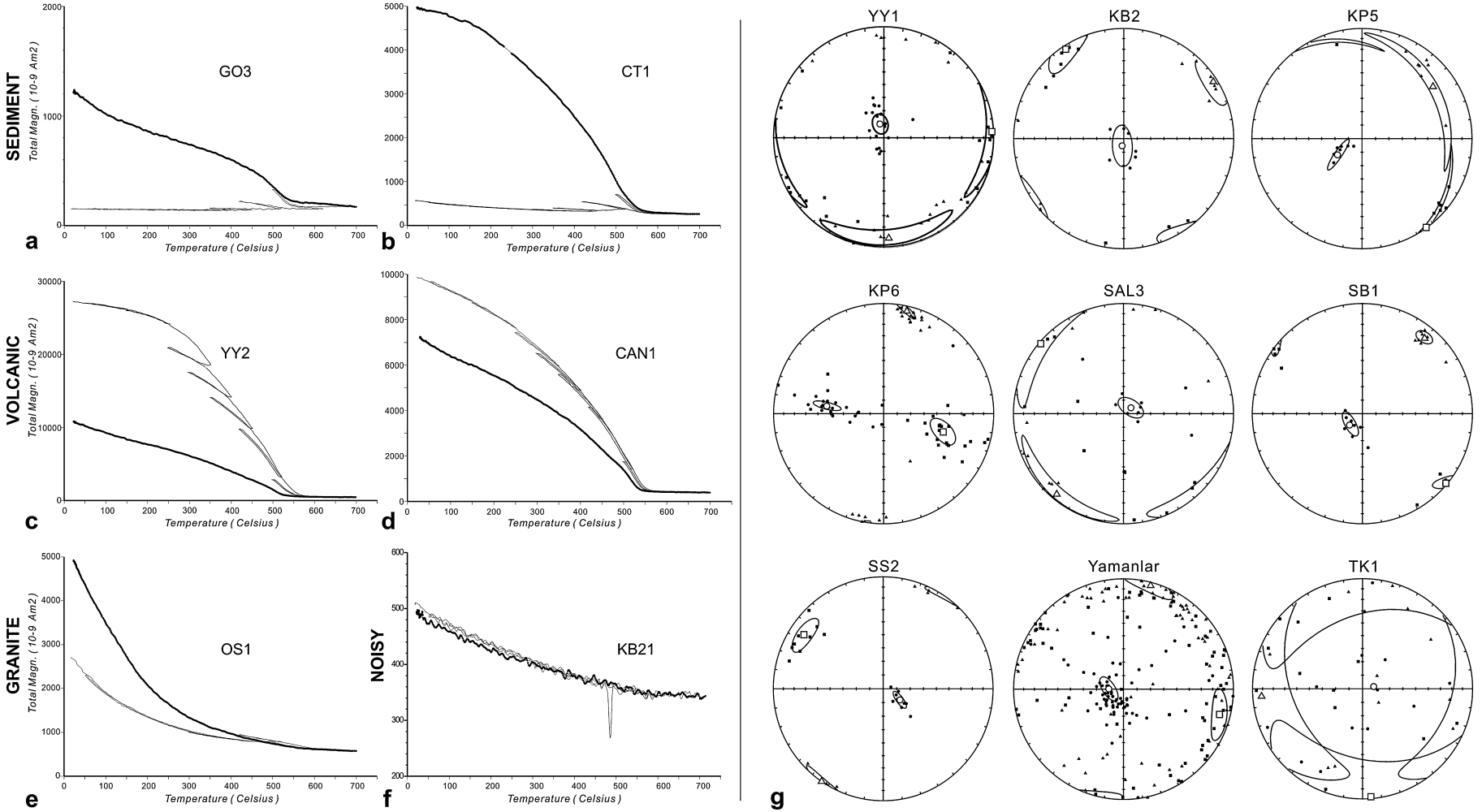

Fig. 4. (a–f) Thermomagnetic curves (on a Curie balance) generated with the segmented heating protocol (Mullender et al., 1993) for representative samples from sedimentary (a–b), volcanic (c–d) and granitic (e) rocks. A noisy appearance is indicative of a weak magnetic signal (f). The final cooling segment is indicated with the thicker black line. (g) Equal area projections of the anisotropy of the magnetic susceptibility (AMS) for representative locations with circles/squares/triangles as $k_{min}/k_{int}/k_{max}$ and their error ellipses after bedding plane correction (Jelinek, 1981).

itive reversal test ($\gamma = 10.0° < \gamma_c = 14.2°$, classification C). The result of the 6 sites on average shows a significant clockwise rotation of $20 \pm 10°$. The middle–late Miocene results from this locality are quite dispersed, however, resulting in a large error interval, and the locality mean shows a counter-clockwise rotation (CCW) of $-23 \pm 27°$. Two sites have mixed polairities with either a positive (KB12, $\gamma = 7.2° < \gamma_c = 14.6°$, classification C) or indeterminate (KB11, $\gamma = 10.6° < \gamma_c = 29.2°$) reversal test (Figs. 5 and 6, Appendix 2). Yet, there are two distinct rotation values for the two age intervals. As we will see below, these mean rotations are

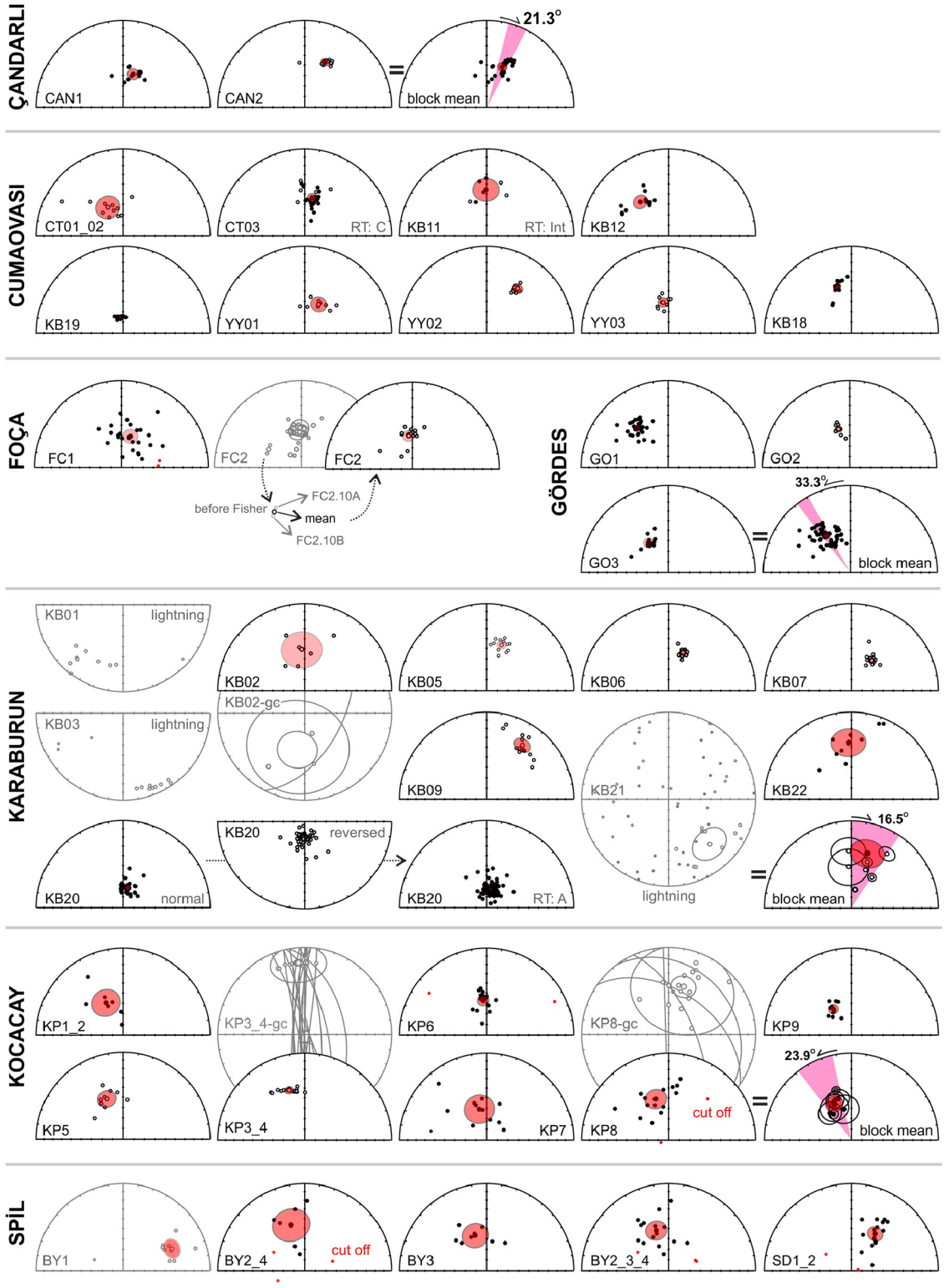

Fig. 5. Equal area projections of the ChRM directions for all sites. Open (closed) symbols denote projection on upper (lower) hemisphere. Large black symbols with red-transparent circle indicate respectively the mean directions and their cone of confidence (α_{95}). Red (small) circles indicate the individual directions rejected after applying a 45° cut-off. Gray lines indicate the great circles (gc) use to calculate the best fitting ChRM directions (McFadden and McElhinny, 1988). Gray equal area projections show rejected sites affected by lightning or very low intensity samples. (For interpretation of the references to color in this figure legend, the reader is referred to the web version of this article.)

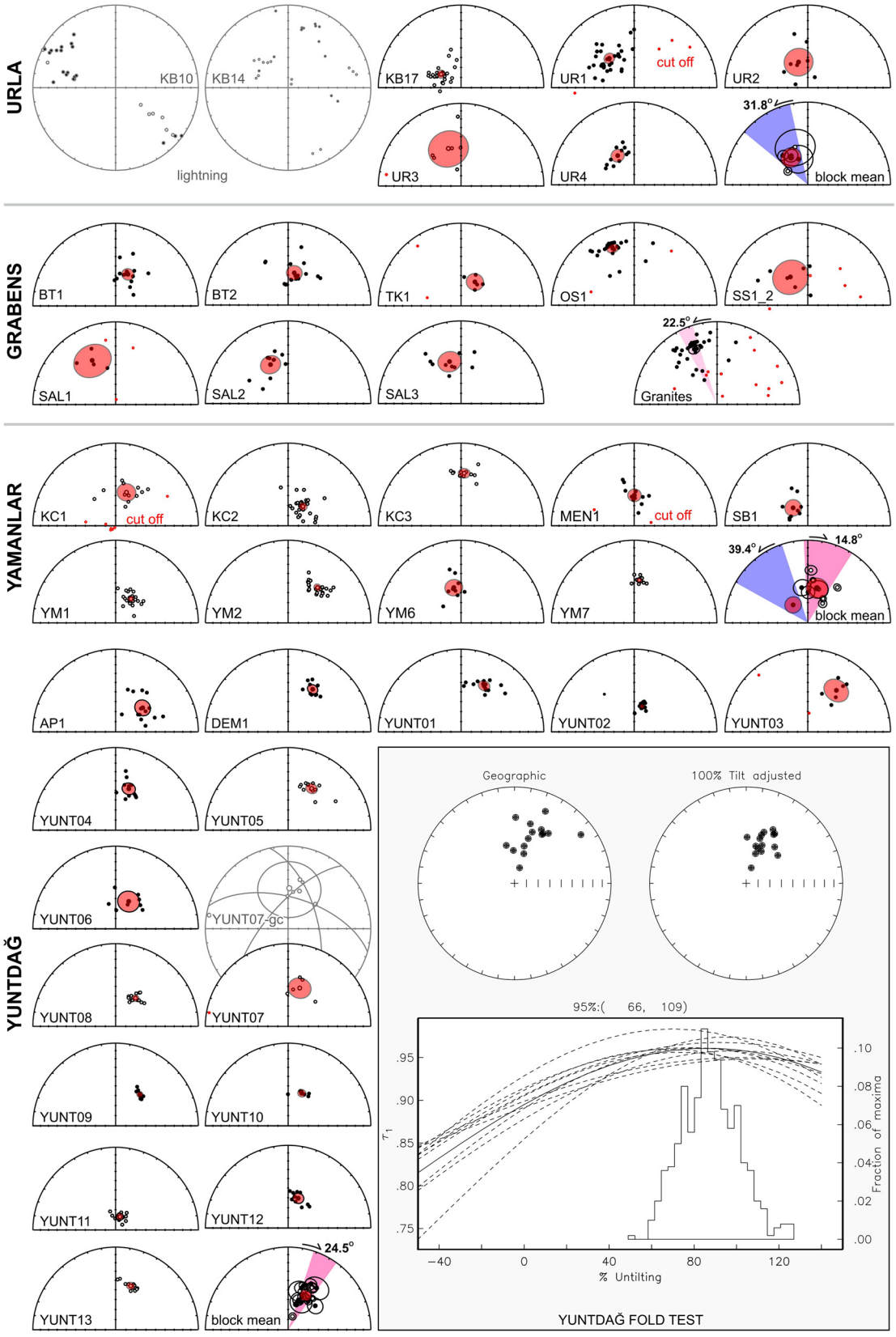

Fig. 5. (*continued*)

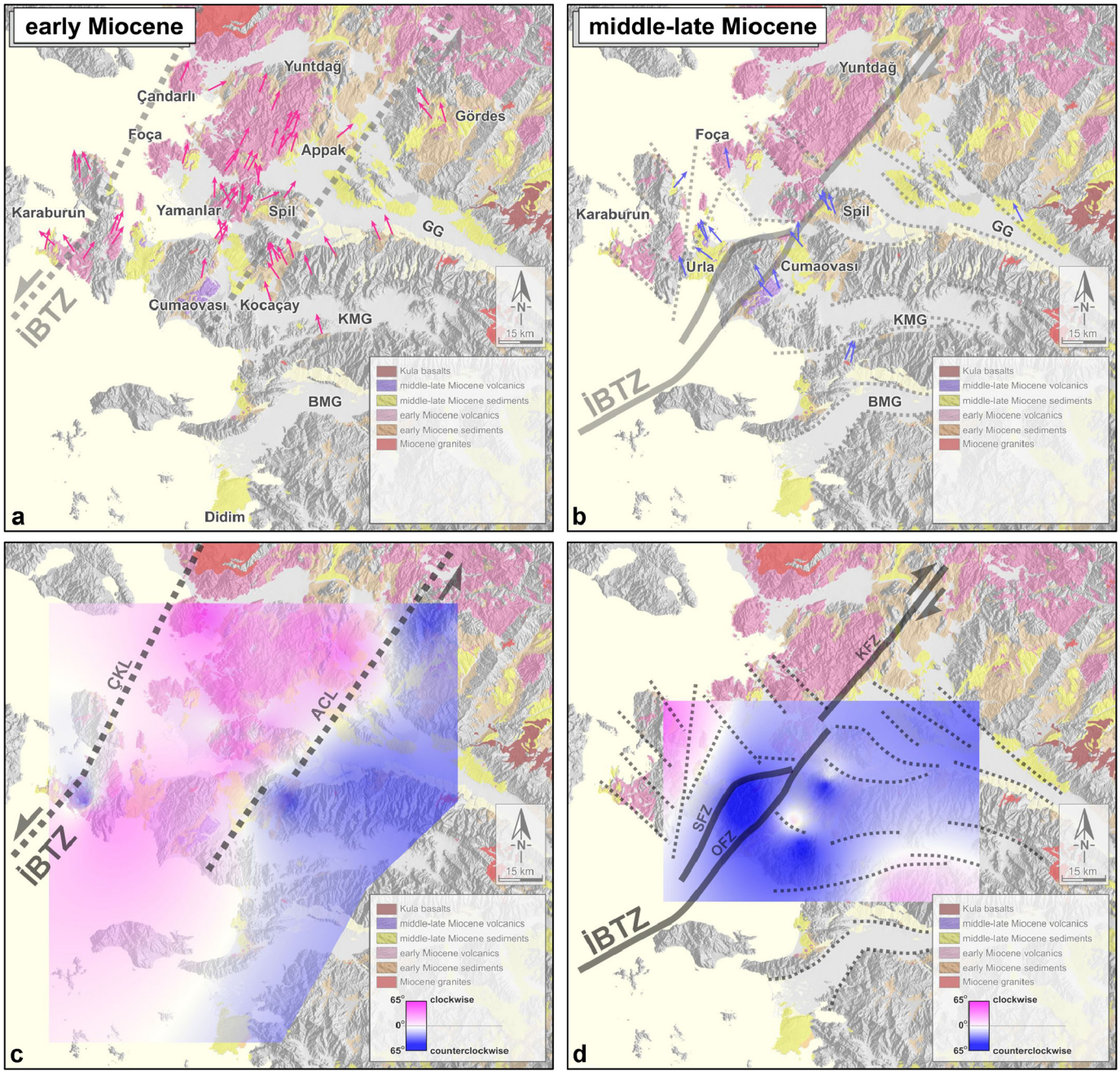

Fig. 6. Paleomagnetic results from this study. The rotation vectors for early Miocene rocks (a) and middle–late Miocene rocks (b) with interpolated rotations for early Miocene (c) and middle–late Miocene (d). Three early Miocene sites (CT1, YY3, YM6) and two middle–late Miocene sites (CT3, BY1) ignored in calculation of interpolated rotation due to the increase of homogeneity of the rotations. GG, Gediz Graben; KMG, Küçük Menderes Graben; BMG, Büyük Menderes Graben; ÇKL, Çandarlı–Karaburun Lineament; ACL, Appak–Cumaovası Lineament; OFZ, Orhanlı Fault Zone; SFZ, Seferihisar Fault Zone; KFZ, Kaleköy Fault Zone.

consistent with those found in the other areas within the İBTZ (Table 1).

From the Foça area within the İBTZ, the early Miocene result from one sedimentary site (FC1) reveals a clockwise rotation of $16 \pm 12°$, while the volcanic rocks of early Miocene age (FC2) are rather scattered and document a (not significant) counter-clockwise rotation of $-7 \pm 11°$ (Figs. 5 and 6, Table 1).

The Karaburun East area lies within the İBTZ has 4 volcanic sites (KB05, KB06, KB08 and KB09 in Fig. 2) that consistently show reversed directions (Fig. 5). The mean locality result documents a significant clockwise rotation of $27 \pm 15°$ (Table 1).

The Kocaçay basin, which is located adjacent to the eastern rim of the İBTZ, has 7 sites of early Miocene age (Fig. 2), of which 3 have normal and 3 have reversed polarity (Fig. 7 and Appendix 2). One site (KP9) has both polarities, with a positive reversal test ($\gamma = 9.0° < \gamma_c = 16.0°$, classification C). But also the means of the normal and reversed sites from this locality provide a positive reversal test ($\gamma = 7.7° < \gamma_c = 18.1°$, classification C). The mean for this locality shows a counter-clockwise rotation of $-24 \pm 9°$, contrary to what we generally see for the early Miocene localities within the İBTZ (Fig. 6 and Table 1).

The Spil area comprises 6 sampling sites (Figs. 2 and 5), two of early Miocene age, and four of middle–late Miocene age. For the early Miocene, we combined two sites (SD1-2), which gives a rather large clockwise rotation of $33 \pm 8°$. The middle–late Miocene sites give on average a counter-clockwise rotation of

Table 1
Block mean paleomagnetic results from this study and the available published data of Kissel et al. (1987), Beck et al. (2001), van Hinsbergen et al. (2010), Uzel et al. (in preparation). N_c, number of samples used for the mean after application of a fixed cut-off (45°); D, declination; I, inclination; ΔD_x, corresponding error in declination. Here, we determine virtual geomagnetic pole (VGP) distribution statistics (K, A95) and the corresponding error in declination (ΔD_x). $A95_{min}$ and $A95_{max}$ correspond to the confidence envelope of Deenen et al. (2011, 2014): if A95 falls within this envelope the distribution likely represents paleosecular variation. If A95 < $A95_{min}$ the distribution is too tight and represents a spot-reading of the field, as is indicated for a number of volcanics sites.

Basin/Locality	N_c	D	I	ΔD_x	K	$A95_{min}$ < **A95** < $A95_{max}$
Western side of İBTZ/early Miocene						
Chios (4)	89	348.1	61.0	6.1	16.5	3.0 < 4.7 < 4.5
Karaburun West	4	171.8	−54.1	30.3	15.0	6.9 < 21.0 < 34.2
Lesbos (3)	60	5.2	49.7	6.3	13.4	3.4 < 5.4 < 6.2
Ayvalık-Bergama (3)	25	5.5	49.6	9.6	14.3	4.6 < 8.3 < 11.3
mean	***4***	***358.5***	***53.8***	***12.7***	***78.2***	6.9 < **10.5** < 34.2
Inside of İBTZ/early Miocene						
Bergama (1)[a]	28	21.3	38.6	6.8	22.5	3.2 < 6.3 < 10.5
Çandarlı	26	21.3	49.2	5.4	37.9	4.6 < 4.7 < 10.5
Cumaovası	6	19.7	51.0	10.1	22.2	5.9 < 24.0 < 26.5
Foca	26	15.6	59.7	11.5	11.6	3.3 < 8.7 < 10.5
Karaburun East	4	207.2	−44.4	15.2	46.5	6.9 < 13.6 < 34.2
Kocaçay	7	336.1	53.2	9.4	61.3	7.8 < 7.9 < 24.1
Spil	16	33.1	48.3	8.3	26.9	5.6 < 7.2 < 14.3
Yamanlar	9	17.5	53.2	12.6	19.0	5.0 < 12.1 < 20.5
Yuntdağ	17	24.2	51.4	7.3	34.2	3.9 < 6.2 < 13.8
mean (without Bergama and Kocaçay)	***7***	***23.1***	***51.2***	***6.0***	***141.6***	**5.1** < A95min(5.5)
Inside of İBTZ/middle–late Miocene						
Cumaovası	4	337.0	51.8	26.8	17.8	6.9 < 22.4 < 34.2
Foca	17	173.5	−58.5	10.5	25.5	3.9 < 7.2 < 13.8
Spil	15	342.6	50.0	12.1	14.5	5.8 < 10.4 < 14.9
Urla	4	334.6	48.8	8.3	113.5	6.3 < 7.2 < 29.7
Yamanlar	9	320.6	67.0	17.9	21.0	5.0 < 11.5 < 20.5
mean	***5***	***338.1***	***55.2***	***11.4***	***53.6***	5.9 < **9.2** < 26.5
Eastern side of İBTZ/early Miocene						
Gediz Graben	16	338.9	43.0	10.1	17.2	4.0 < 9.1 < 14.3
Gördes	43	322.8	46.3	3.6	47.6	2.7 < 3.2 < 7.7
Granites	34	338.1	32.7	6.0	19.3	2.9 < 5.7 < 8.9
NE-trending basins (3)	40	13.4	52.7	9.2	10.2	3.9 < 7.7 < 9.1
Söke (5)	122	352.1	53.2	3.6	19.5	2.5 < 3.0 < 4.0
Zeytinçayı (2)[b]	121	332.3	50.6	11.3	91.8	6.9 < 9.6 < 34.2
mean (without NE-trending basins)	***6***	***337.0***	***47.3***	***10.2***	***57.0***	5.9 < **8.9** < 26.5
Eastern side of İBTZ/middle–late Miocene						
Büyük Menderes Graben	34	15.8	57.0	7.3	19.4	2.9 < 5.7 < 8.9
Eycelli (2)[c]	52	32.4	45.0	6.9	12.3	2.6 < 6.2 < 7.2
Gediz Graben	10	344.4	46.1	13.4	17.4	4.8 < 11.9 < 19.2
Küçük Menderes Graben	5	30.1	62.6	17.1	40.1	6.3 < 12.1 < 29.7
Söke (5)	6	20.9	48.5	11.4	46.7	8.3 < 9.9 < 26.5
mean (without Gediz Graben)	***5***	***24.9***	***53.5***	***14.1***	***63.5***	6.9 < **11.6** < 34.2

[a] Parametric bootstrap resampling from Kissel et al. (1987).
[b] Taken from Şen and Seyitoğlu (2009).
[c] Parametric bootstrap resampling from Şen and Seyitoğlu (2009).

$-17 \pm 12°$ (Fig. 6 and Table 1). We discard the volcanic site BY1 since it presents the spot reading.

In the Urla basin 9 sites were sampled, all of middle–late Miocene age. During the measurements it was realized that three sites (KB10, KB14 and KB15 in Fig. 2) were affected by lightning, as can be seen by unusually high intensities and the typical very rapid decay at low AF demagnetization steps; another site (KB17) also showed lightning-induced effects but was later carefully re-sampled as UR5 (Appendix 2). The accepted volcanic sites (UR2–5) show a ChRM removed at fields between 20 and 60 mT and temperatures between 300–580 °C, while the sedimentary site (UR1) reveals a ChRM in magnetic fields ranging 15–45 mT and temperatures of 120–380 °C (Fig. 4). These five remaining sites give a consistent counter-clockwise average rotation of $-25 \pm 8°$ (Figs. 5 and 6, Table 1).

The Yamanlar area has 11 early Miocene sites in both volcanics and sediments (Fig. 2). Several volcanic sites record only a single spot reading of the field (A95 < $A95_{min}$) and occasionally two spot readings are found in one site (e.g. YM2) (Appendix 2). The average locality direction documents a well-determined clockwise rotation of $18 \pm 13°$ (Fig. 5, Table 1). Only one (sedimentary) site of middle–late Miocene age was sampled and shows a counter-clockwise rotation of $-39 \pm 18°$ (Fig. 6 and Appendix 2).

In the Yuntdağ area, all 17 sites are of early Miocene age, and most consist of volcanic rocks (Fig. 2). Typically, many volcanic sites record one or two spot readings of the field, as can be derived from the A95 criteria (Appendix 2). A few sedimentary sites (AP2 and AV1) did not yield any sensible results because of very low intensities. In total, we have 17 results of mixed sedimentary and volcanic origin, but there is a very distinct and consistent clockwise rotation of $24 \pm 7°$ (Figs. 5 and 6, Table 1).

3.2. Paleomagnetic results outside the İBTZ

Outside the İBTZ, we consider two separate regions, the area to the west and to the east of the İBTZ, since the paleomagnetic results of the two areas differ significantly, especially in the sense of the amount of data (Fig. 2).

In the area west of the İBTZ, we have sampled only one area with sufficient paleomagnetic data, Karaburun West (Figs. 2 and 5).

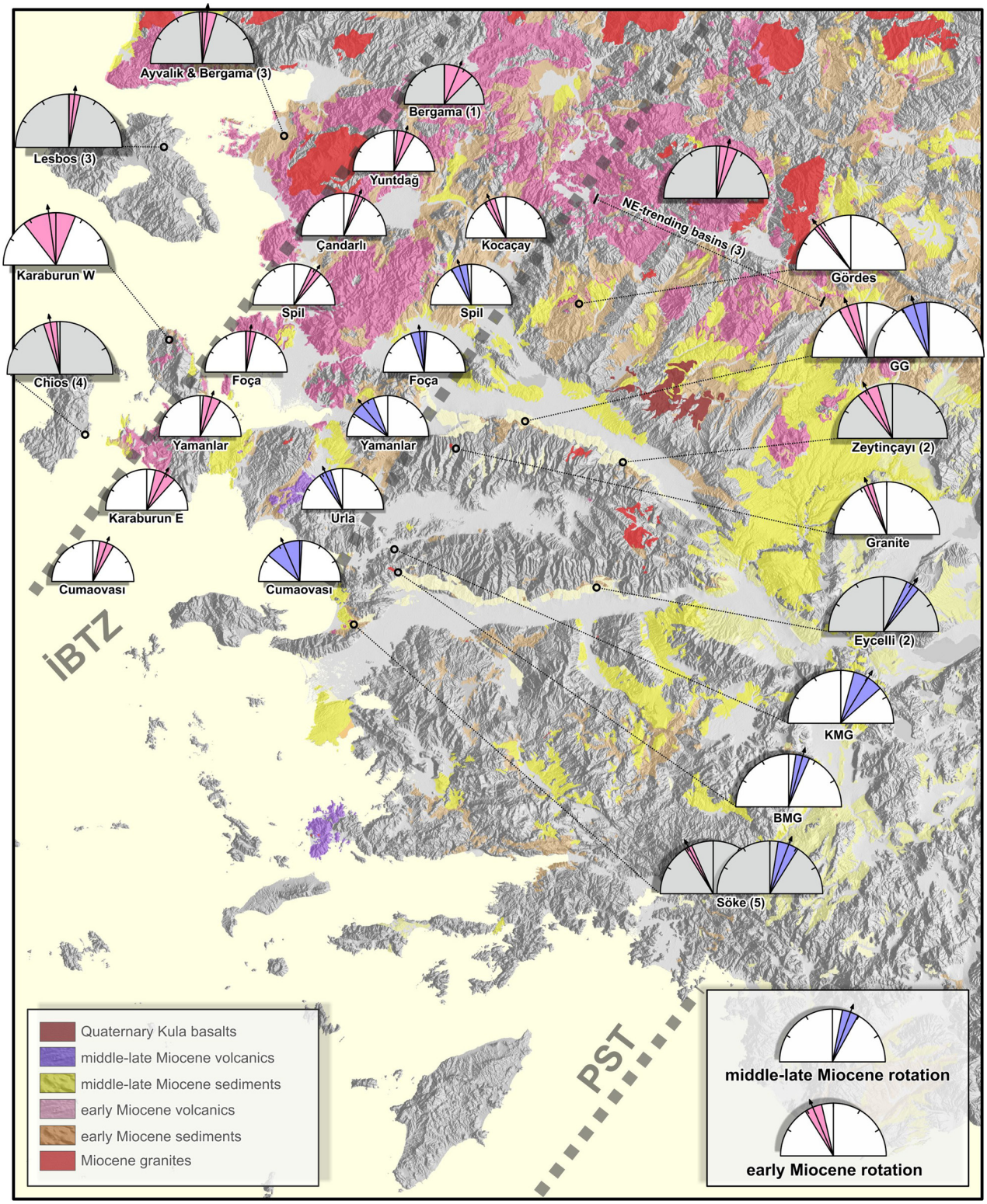

Fig. 7. Paleomagnetic data from this study and previous paleomagnetic studies. Numbers between brackets refer to (1) Kissel et al. (1987); (2) Şen and Seyitoğlu (2009); (3) van Hinsbergen et al. (2010a); (4) Kaymakci et al. (2007); (5) Uzel et al. (in preparation).

Quite a few sites (KB01, KB03-04, KB21, and KB23) from this area were affected by lightning, or suffered from random directions ('shotgun pattern') and hence did not yield any reliable results. We sampled an extensive red bed sequence (KB20, more than 90 levels), which showed both normal and reversed polarities (Appendix 2), and a positive reversal test ($\gamma = 2.8° < \gamma_c = 3.2°$, classification A). All together only 4 sites gave good results and their mean shows a large scatter and no significant rotation for this western Karaburun area: $-8 \pm 30°$ (Figs. 5 and 6, Table 1).

In the area east of the İBTZ we have been able to sample appreciably more areas successfully. The results from the areas of the E–W-trending Küçük Menderes and Büyük Menderes Grabens, show only clockwise rotations in late Miocene rocks of $32 \pm 7°$ and $16 \pm 7°$, respectively. Granites of early Miocene age were

also sampled in the graben area and gave good results from 3 sites that record a counter-clockwise rotation of $-22 \pm 6°$. In the Gediz Graben we find both two early Miocene sites recording a counter-clockwise rotation of $-21 \pm 10°$ and a middle–late Miocene counter-clockwise rotation of $-16 \pm 13°$. In the NE-trending Gördes basin early Miocene sediments at 2 sites (together at 43 levels) record a counter-clockwise rotation of $-37 \pm 4°$ (Figs. 5 and 6, Table 1).

4. Discussion

Previous studies (Kaya, 1981; Sözbilir et al., 2011; Uzel et al., 2012, 2013) show that the study area comprises two well-defined stratigraphical sequences separated by a major unconformity. The older one was informally named *lower sequence* (early Miocene, 21–16 Ma; Uzel et al., 2013), while the younger was named *upper sequence* (middle to late Miocene, 13.2–5.3 Ma; Uzel et al., 2013). Stratigraphical relationships and kinematic results indicate that these sequences belong to at least two different deformation phases. We are now able to add our new paleomagnetic data to the evidence derived from earlier structural studies. We will incorporate new $^{40}Ar/^{39}Ar$ ages, which are now being acquired (to be published in a subsequent paper). In the following we discuss the two major phases separated by the major unconformity, the early Miocene and the middle–late Miocene.

4.1. First stage: the early Miocene

In the early Miocene, we distinguish three domains, based on structural evidence and our new paleomagnetic results: (1) the first domain comprises the area west of the İBTZ, i.e. to the west of the Çandarlı–Karaburun line; (2) the second domain corresponds to the transfer zone itself, which according to Uzel et al. (2013) is delimited in the west by the Karaburun–Çandarlı line, and in the east by the Söke–Gördes line; (3) hence the third domain is the area to the east of Söke–Gördes line (the domain boundaries are denoted by dashed lines in Figs. 6 and 7).

Our only locality in the first domain is Karaburun West, which shows no significant rotation, certainly considering the large error envelop ($-8 \pm 30°$, Fig. 7). Also other studies do generally not provide robust evidence for significant net rotations since the early Miocene. Kondopoulou et al. (2011) published results from the island of Chios, from early–middle Miocene (mammal zone MN5) sedimentary units, which corresponds approximately to the *lower sequence*. They document a CCW rotation of $-12 \pm 5°$ by combining all normal and reversed polarity data (Fig. 7 and Table 1). However, a reversal test is not reported (mean normal and reversed directions are not given separately), but glancing at their Fig. 9 the test is most likely negative. Because of some anomalous lava directions on Chios, they speculate that Chios is most likely part of a zone of chaotic rotations that includes the west Anatolian Karaburun peninsula and the Dikili, Foça and Yuntdağ volcanic regions. This hypothesis does not fit with our observations, as we will discuss below. In Lesbos, numerous lava flows have been sampled and published by Kissel et al. (1987) and Beck et al. (2001). These results have been re-analyzed by van Hinsbergen et al. (2010b) and they argued that the early Miocene rotations of Lesbos are insignificant and they range between $-5 \pm 6°$. Furthermore, new results from 25 lava flows in the Ayvalık-Bergama region reported by van Hinsbergen et al. (2010a) show a non-significant rotation of $-6 \pm 10°$. If we combine our Karaburun West results with the published data, we conclude that the entire early–middle Miocene sequence below the middle Miocene unconformity, in the region, west of the İBTZ shows no significant net rotation since the early Miocene: $-1 \pm 13°$ (Fig. 7 and Table 1). This does not necessarily imply that no rotations have taken place, since the net zero rotation may in principle be the sum of any combination of CW and equally large CCW rotations. In summary, the relatively consistent results from the western part of the İBTZ do not support a "region of chaotic rotations" proposed by Kondopoulou et al. (2011).

The results from the second domain, the İBTZ zone proper, are remarkably consistent. If we combine our Early Miocene results (Fig. 7 and Table 1), we find an average net rotation since the early Miocene of $23 \pm 6°$. We have not included the results of Kocaçay Basin (see Table 1) although the Kocaçay site was assumed to be of early Miocene age. However, the results are in remarkably good agreement with the early Miocene rotations of the third domain, east of the İBTZ. It must be noted that the Kocaçay locality is at the very edge of the İBTZ, and would fit better in the latter domain. Our average rotation of $23 \pm 6°$ for the İBTZ, also fits with some results from Kissel et al. (1987), from 3 sites in the Bergama region. Parametric (Monte Carlo) bootstrap resampling of their published sites and parameters gives a best estimate of $21 \pm 7°$ CW. Including this result does therefore not change our conclusions. Kissel et al. (1987) also published some results from sites near Dikili, Ayvalık, and Yuntdağ, but we cannot use them because individual site locations were not given; moreover, their individual sites appear to belong to other and different blocks/localities than we prefer to use.

The results from the third domain, east of the İBTZ, are again and similarly remarkably consistent and document on average a CCW rotation of $-23 \pm 13°$ ($N = 5$). If we assume that Kocaçay also belongs to this domain, this rotation does not change ($-23 \pm 10°$, $N = 6$). A CCW rotation published by Şen and Seyitoğlu (2009) from the early Miocene location of Zeytinçayi ($-28 \pm 11°$) is in excellent agreement with our results. However, our results are incompatible with the CW rotation derived by van Hinsbergen et al. (2010a) for the NE trending basins north of the Gediz Graben, which they called the Northern Menderes Massif. They sampled numerous localities—all north of our localities with the exception of Gördes—and found a CW rotation of $13 \pm 9°$ based on a compilation of 40 lava flows from several sites (Fig. 7 and Table 1).

In summary, for the early Miocene we find a consistent rotation regime in all three domains. To the west of the İBTZ we find no significant rotations recorded in early Miocene rocks, within the İBTZ proper we find a consistent regime of on average 23° CW rotation, while in east of the İBTZ there is an equally consistent regime of on average 23° CCW. This implies a total differential rotation between the two latter areas of 46° since the early Miocene. Clearly, this must be evaluated in the context of the later rotational history, as we will discuss below.

4.2. Second stage: the middle–late Miocene

In the middle–late Miocene—which marks the *upper sequence* above the major middle Miocene unconformity (Kaya, 1981; Genç et al., 2001; Sözbilir et al., 2011; Uzel et al., in preparation, 2012, 2013)—we can only distinguish two domains (2 and 3) in our paleomagnetic discussion. In domain 1 we have not been able to acquire reliable paleomagnetic data because of the lack of suitable outcrops. Only one study by Avigad et al. (1998) reports a CW rotation from Tinos Island, to the southwest of Chios. Hence, we can only present new paleomagnetic data for domains 2 and 3.

For both domains, we again see a remarkably consistent pattern for our middle–late Miocene paleomagnetic data (Figs. 6 and 7). This time, however, there is a clear role reversal: the rotation pattern within the İBTZ area is consistently counter-clockwise; while east of the İBTZ there is a consistent clockwise pattern. Moreover, it is of a similar magnitude as the rotation observed in our early Miocene data. From our 5 middle–late Miocene localities within the İBTZ we find an average of $-22 \pm 14°$ CCW, while in the

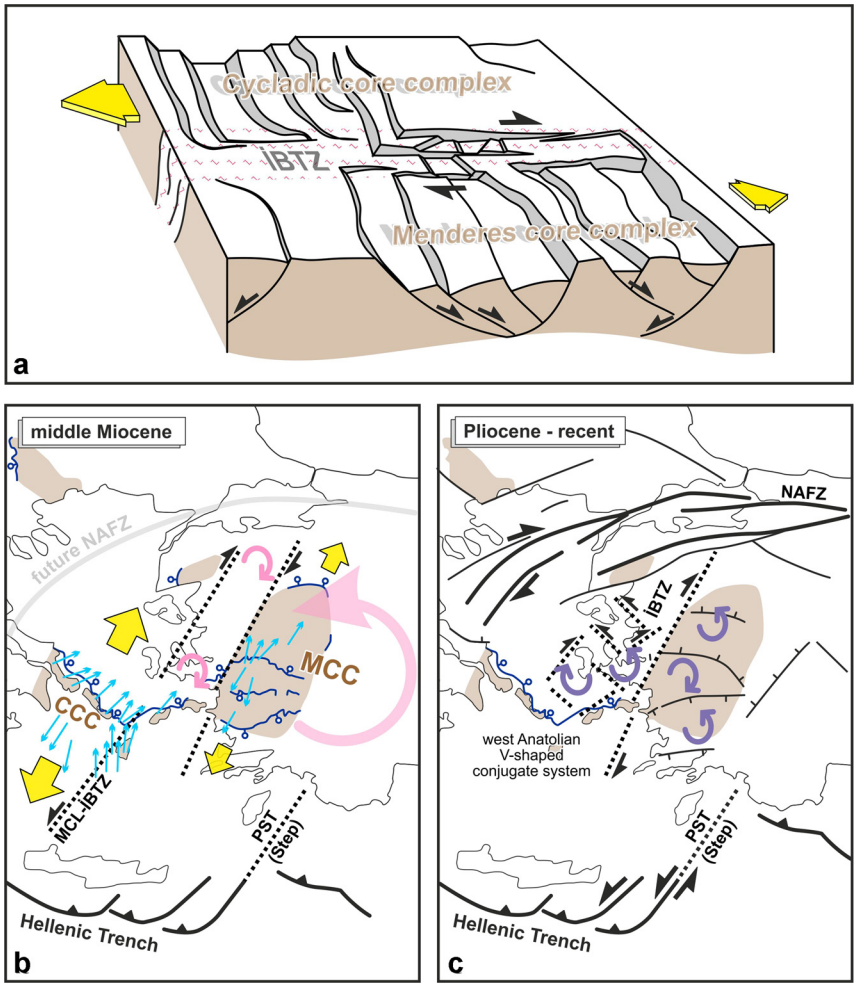

Fig. 8. Configuration of geodynamic elements and simplified pattern of the present-day extension directions in the west Anatolian and Aegean region (compiled from Barka, 1984; Reinecker et al., 2005; Uzel et al., 2013; Kaymakci, 2006 and this study). a) Simplified model depicting differential stretching between the Cycladic Core Complex (CCC) and the Menderes Core Complex (MCC) that facilited by the İzmir-Balıkesir Transfer Zone (İBTZ). Differential extensions and related rotations during the b) middle and c) Pliocene to recent. MCL, Mid-Cycladic Lineament; NAFZ, North Anatolian Fault Zone; PST, Pliny-Strabo Trench.

eastern area we find a consistent average of $25 \pm 14°$ CW for 4 localities including the Eycelli road section of Şen and Seyitoğlu (2009). Although, Şen and Seyitoğlu (2009) argued that this locality is early Miocene in age, but the obtained rotations from the locality supports the late Miocene age proposed originally by Sözbilir and Emre (1990).

Remarkably, there is again a very similar differential rotation of 47° between the two areas but now in an opposite sense (Figs. 6 and 7). The paleomagnetic data we have presented picture a clear scenario for the major transfer zone represented by the İBTZ. Both volcanic and sedimentary rocks from the early Miocene in the İBTZ and east of it, have undergone major and opposite rotations since then. Between the early and middle–late Miocene the İBTZ experienced a $23° + 22° = 45°$ CW rotation, while in the same time interval the area east of the İBTZ rotated $23° + 25° = 48°$ CCW. Surprisingly, the rotations are within error identical but senses are opposite (Fig. 6). Since the late Miocene, the İBTZ rotated 22° CCW (yielding the net 23° CW rotation observed for the early Miocene). But, since then the eastern area of the İBTZ rotated 25° CW (yielding the 23° CCW rotation for the early Miocene).

4.3. Regional implications of rotations

As seen in Fig. 6, the boundary of İBTZ is very well defined by the early Miocene rotations where the boundary of CW and CCW rotations is sharply separated. However, the eastern boundary of the İBTZ for its middle–late Miocene configuration does not correspond to the boundary of domains of clockwise and counterclockwise rotations, while the western boundary of the İBTZ is still recognizable. A possible explanation for this change may be related to the evolution of the İBTZ from a large shear zone in the early Miocene into a narrow discrete zone in the late Miocene (Uzel et al., 2013). Such behavior is common for shear zones (e.g. Naylor et al., 1986), provided that strain softening is associated with the deformation, for example facilitated by heat generated by the ascending magmatic material during the middle Miocene (Fig. 8a).

The İBTZ is a NE–SW trending strike-slip shear zone that delimits the western margins of the E–W striking horst–graben complex of west Anatolia that defines the locus of maximum extension. These E–W grabens include from north to south Gediz, Küçük Menderes and Gediz grabens. The İBTZ has been recognized previously (Uzel et al., 2013) and was interpreted as the NE continuation of the Mid Cyladic Lineament (MCL) (Walcott and White, 1998; Pe-Piper et al., 2002). It marks the boundary between the eastern and western Aegean domains (Morris and Anderson, 1996). The MCL ceased to be active in the latest Miocene–Early Pliocene coevally with the development of the North Anatolian Fault (Walcott and White, 1998). Regional kinematic studies have also suggested that a major change in the kinematics of the Aegean occurred in the latest Miocene–early Pliocene (Le Pichon et al., 1995). These structures played a major role in the exhumation of

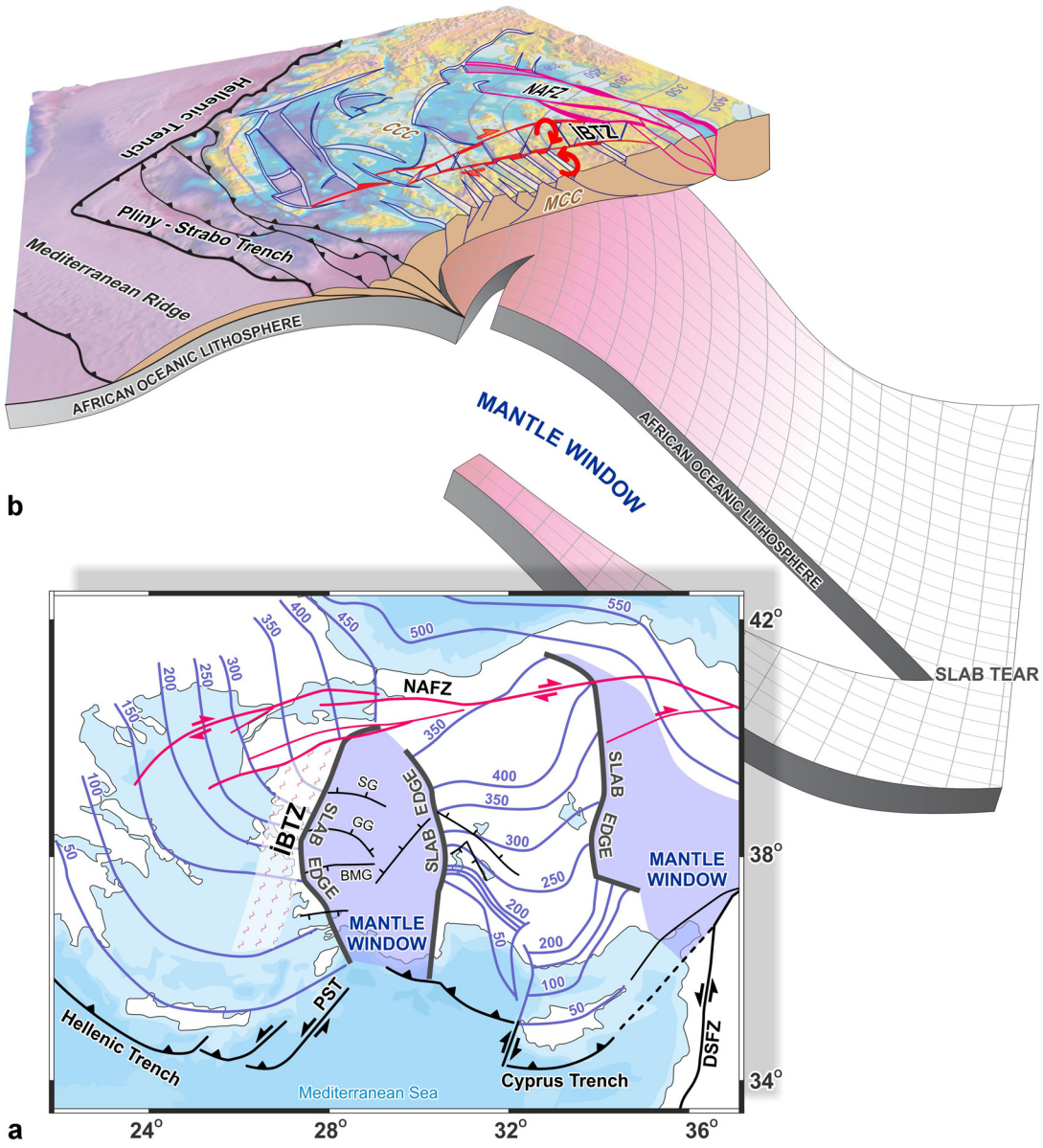

Fig. 9. a) Generalized tectonic map showing the contours (in km) of the Aegean and the Cyprean slabs with major structural elements of the area (Biryol et al., 2011). b) Simplified surface to mantle 3D model of Aegean–west Anatolian region (modified from Faccenna et al., 2006; van Hinsbergen et al., 2010; Biryol et al., 2011; Gessner et al., 2013; Jolivet et al., 2013) depicting differential rotations along İBTZ. The main possible driving mechanism for the vertical axes rotations driven by the differential stretching along İBTZ is related to slab detachment and slab tear (STEP fault) processes at the northern edge of subducting African slab.

MCC. While the different studies agree on the kinematics and driving forces, however, there is still debate whether this exhumation is related to a single phase of extension (Seyitoğlu and Scott, 1992; Seyitoğlu et al., 1992), or to two phases (Sözbilir and Emre, 1996; Koçyiğit et al., 1999; Lips et al., 2001; Sözbilir, 2001, 2002; Bozkurt and Sözbilir, 2004).

According to our paleomagnetic data, the region to the east of the İBTZ—which corresponds mainly to the MCC region—underwent a counterclockwise rotation during the middle Miocene (Avigad et al., 1998), contemporaneously the areas within the İBTZ rotated in opposite sense (Fig. 6). Here, the rotation sense and amount of the MCC region was mostly uniform suggesting that the exhumation of the MCC most likely be related to orthogonal extension. This implies that the rotations related to exhumation of the core of the MCC occurred as "rigid-body" rotation, i.e. without major internal rotational deformation or pure shear deformation. In addition, the stretching lineations of Jolivet et al. (2010 and references therein) from both MCC and CCC are also in support of this rigid body rotation (Fig. 8b).

Clockwise rotations within the İBTZ and counterclockwise rotations of the surrounding blocks suggest that the İBTZ was a dextral shear zone during the early Miocene. By accommodating the Miocene extension, the İBTZ and MCL collectively have played an important role in the tectonics of the region and the exhumation of MCC. Both the end of the activity of the MCL and a concurrent major change in the rotations/kinematics of the Aegean occurred during the latest Miocene–early Pliocene and is related to initiation of the North Anatolian Fault Zone and westwards escape of Anatolian Plate (Fig. 8c).

Surface observations of Gessner et al. (2013) and mantle tomography images of van Hinsbergen et al. (2010) and Biryol et al. (2011) suggest there are major differences in the upper mantle and lithosphere behavior of the region between the MCC and the area to the west (Fig. 9). Additionally, geochemical analyses of Miocene volcanism suggest that the thickness of the lithosphere beneath

western Anatolia is significantly different under the MCC and the İBTZ: it is thinning from east to west. In addition, the nature of the volcanism also changed from shoshonitic and ultrapotassic to high potassic affinity (Genç et al., 2001; Aldanmaz et al., 2000; Pe-Piper et al., 2002; Altunkaynak et al., 2010), as the strike-slip tectonics became dominant. In addition, the spatial distribution of the Miocene volcanic rocks and their eruption centers indicate that volcanic activity was constrained to the NE-trending İBTZ as a conduit for magmas to reach the surface (Fig. 2). All these lines of evidence suggest that the İBTZ not only separated two core complexes, the MCC and the CCC, but also a deep seated structure related to tear along the subducted northern edge of the African slab with the characteristics of a STEP fault as suggested by van Hinsbergen et al. (2010) (Fig. 9).

4.4. Regional implications of İBTZ

The fault geometry presented here is kinematically similar to, for example, the late Cenozoic conjugate strike-slip fault system in central Tibet along the India–Asia collisional system (Taylor et al., 2003; Yin and Taylor, 2011). Such fault systems are explained by two sets of Riedel shears. A similar conjugate fault system is documented from Turkey at the Eastern Anatolian conjugate system (Yin, 2010; Yin and Taylor, 2011; Koç and Kaymakci, 2013) where a northern right-lateral system (NAFZ in Fig. 1) and a southern left-lateral system (EAFZ in Fig. 1) experience north–south contraction. This type of mechanism has been accepted as paired general shear deformation, which cannot be explained by the Coulomb Failure criterion (Yin and Taylor, 2011). As first identified from the central Tibet conjugate fault zone (Taylor et al., 2003) they lie where the maximum principal stress (σ_1) direction is the obtuse bisetrix (60–75°). This is in contrast to the X-shaped shear fractures where σ_1 is the acute bisetrix (30°) and the fault zones obey the Coulomb Failure Criterion.

According to Kahle et al. (2000) subduction rates within the Hellenic system vary along the trench and through time. This variation along the Hellenic trench is explained by laterally bounded subduction transform edge propagator faults (STEP; Govers and Wortel, 2005; Biryol et al., 2011). Recent seismic anisotropy studies by Paula et al. (2014) provided supporting evidence for the slab rollback in the Aegean Sea and a mantle window beneath southwestern Anatolia (Fig. 9b).

Based on the differences in extension geometry and metamorphic history between Samos and western Anatolia an early Miocene (or older) tectonic boundary between the Aegean and Anatolian domains has already been proposed (e.g. Ring et al., 1999; 2010; Okay, 2001). However, the name of the İBTZ was firstly added to the literature by Sözbilir et al. (2003) as an intermittently active NE–SW trending and strike-slip dominated shear zone bounding the E–W trending supradetachment basins and MCC in western Anatolia. More recently, several field-based studies have documented on the stratigraphic and structural features of the zone (see Uzel and Sözbilir, 2008; Özkaymak and Sözbilir, 2008; Özkaymak et al., 2013; Sözbilir et al., 2011; Uzel et al., in preparation, 2013). These studies all suggested that this seismically active NE-trending corridor of crustal deformation represents the transfer zone between the Aegean and Anatolia. Gessner et al. (2013) suggested that the İBTZ is a surface expression of a tear in the subducting African Slab, named as the West Anatolia Shear Zone. This zone links the North Anatolian Fault zone to the Hellenic trench and shows a sharp vertical boundary between the fast, cold and dense slab below the Aegean and a slow, hot and buoyant asthenospheric region below western Turkey (Fig. 9). This mechanism may also be responsible from southwestward younging volcanism along the İBTZ.

It is important to note that a recent example of conjugate faulting was observed at the Sığacık Gulf, 50 km southwest of İzmir, during the October 2005 earthquake. The aftershock activity was clustered in two distinct zones, striking NW–SE left-lateral and NE–SW right-lateral, respectively, forming a well-defined V-shaped-conjugate strike slip system (Aktar et al., 2007).

5. Conclusions

In this paleomagnetic study, more than 1100 cores from 87 sites have been analyzed to characterize the deformation pattern and kinematics of the İBTZ. Based on tectonostratigraphic studies, our new paleomagnetic results and our structural observations, we identify two phases of rotation during the early Miocene (lower sequence) and middle–late Miocene (upper sequence) in the region.

Paleomagnetically, the İBTZ is very well expressed in the *lower sequence* in having a belt of a very consistent CW rotations surrounded by on average no (net) rotation to the west and consistent CCW rotations to the east. However, the spatial distribution of rotation amounts and senses of the *upper sequence* indicate that the İBTZ evolved into a narrow discrete shear zone by the middle Miocene. Almost homogeneous rotations within and on either side of the İBTZ, for both the *lower* and the *upper sequence*, indicate that the region did not experience internal rotational deformation but uniform orthogonal deformation. This disqualifies the connotation of a zone of chaotic rotations.

Our new results do fit the hypothesis of a two-stage rather than a single-stage extension scenario. We also conclude that the observed rotations are not directly related to major detachment faulting, but to the change in extensional regime of western Anatolia. Recent seismic activity with strike-slip focal mechanism solutions indicate that the İBTZ is still active and transfers west Anatolian extensional strain into the south Aegean Sea.

Acknowledgements

This work is a part of the PhD study of Bora Uzel and it is supported by the Scientific and Technical Research Council of Turkey (Research Grant of ÇAYDAĞ-109Y044) and partly by the scientific research project of Dokuz Eylül University (Project No. 2007.KB.FEN.039). We thank Pinar Ertepinar and Onur Sarıoğlu for their assistance during the paleomagnetic field sampling, Mark Dekkers, Maud Meijers, Côme Lefebvre, Arjan de Leeuw and Erhan Gülyüz for collaborating and critical comments on the paleomagnetic measurements. We also thank An Yin, Mike Taylor and an anonymous reviewer for their constructive comments that greatly improved the manuscript. We dedicate this paper to the memory of Tom Mullender who was the brilliant technician of Fort Hoofddijk Paleomagnetic Laboratory.

Appendix A. Supplementary material

Supplementary material related to this article can be found online at http://dx.doi.org/10.1016/j.epsl.2015.01.008.

References

Aktar, M., Karabulut, H., Özalaybey, S., Childs, D., 2007. A conjugate strike-slip fault system within the extensional tectonics of western Turkey. Geophys. J. Int. 171 (3), 1363–1375. http://dx.doi.org/10.1111/j.1365-246X.2007.03598.x.

Aldanmaz, E., Pearce, J.A., Thirlwall, M.F., Mitchell, J.G., 2000. Petrogenetic evolution of late Cenozoic, post-collision volcanism in western Anatolia Turkey. J. Volcanol. Geotherm. Res. 102, 67–95.

Altunkaynak, İ., Rogers, N.W., Kelley, S.P., 2010. Causes and effects of geochemical variations in late Cenozoic volcanism of the Foca volcanic centre, NW Anatolia, Turkey. Int. Geol. Rev. 52, 579–607.

Avigad, D., Baer, G., Heimann, A., 1998. Block rotations and continental extension in the central Aegean Sea: palaeomagnetic and structural evidence from Tinos and Mykonos (Cyclades, Greece). Earth Planet. Sci. Lett. 157, 23–40. http://dx.doi.org/10.1016/S0012-821X(98)00024-7.

Barka, A., 1984. Geology and tectonic evolution of some Neogene-Quaternary basins in the North Anatolian fault zone. In: Ketin Symposium. In: Geol. Soc. of Turkey, pp. 209–227.

Barka, A., 1992. The North Anatolian fault zone. Ann. Tecton. 6, 164–195.

Beck, M.E., Burmester, R.F., Kondopoulou, D.P., Atzemoglou, A., 2001. The palaeomagnetism of Lesbos, NE Aegean, and the eastern Mediterranean inclination anomaly. Geophys. J. Int. 145, 233–245. http://dx.doi.org/10.1111/j.1365-246X.2001.00376.x.

Biryol, C.B., Beck, S.L., Zandt, G., Özacar, A.A., 2011. Segmented African lithosphere beneath the Anatolian region inferred from teleseismic P-wave tomography. Geophys. J. Int. 184, 1037–1057.

Bozkurt, E., 2001. Neotectonics of Turkey—a synthesis. Geodin. Acta 14, 3–30.

Bozkurt, E., Oberhänsli, R., 2001. Menderes Massif (western Turkey): structural, metamorphic and magmatic evolution. Int. J. Earth Sci. 89, 679–882.

Bozkurt, E., Sözbilir, H., 2004. Tectonic evolution of the Gediz Graben: field evidence for an episodic, two extension in western Turkey. Geol. Mag. 141, 63–79.

Brun, J.-P., Sokoutis, D., 2007. Kinematics of the southern Rhodope Core Complex (northern Greece). Int. J. Earth Sci. 96, 1079–1099. http://dx.doi.org/10.1007/s00531-007-0174-2.

Butler, R.F., 1992. Paleomagnetism: Magnetic Domains to Geologic Terranes. Blackwell Publishing, Boston. 195 pp.

Candan, O., Dora, O.Ö., Oberhanslı, R., Çetinkaplan, M., Partzsch, J.H., Warkus, F.C., Dürr, S., 2001. Pan-African high-pressure metamorphism in the Precambrian basement of the Menderes Massif, Western Anatolia, Turkey. Int. J. Earth Sci. 89, 793–811.

Deenen, M.H.L., Langereis, C.G., van Hinsbergen, D.J.J., Biggin, A.J., 2011. Geomagnetic secular variation and the statistics of palaeomagnetic directions. Geophys. J. Int. 186, 509–520.

Deenen, M.H.L., Langereis, C.G., van Hinsbergen, D.J.J., Biggin, A.J., 2014. Erratum to: Geomagnetic secular variation and the statistics of palaeomagnetic directions [Geophys. J. Int. 186 (2011) 509–520]. Geophys. J. Int. 197, 643.

Duermeijer, C.E., Krijgsman, W., Langereis, C.G., ten Veen, J.H., 1998. Post early Messinian counter-clockwise rotations on Crete: implications for the late Miocene to Recent kinematics of the southern Hellenic Arc. Tectonophysics 298 (1–3), 77–89.

Emre, T., Sözbilir, H., 1997. Field evidence for metamorphic core complex, detachment faulting and accommodation faults in the Gediz and Büyük Menderes grabens (Western Turkey). In: International Earth Sciences Colloquium on the Aegean Region IESCA-95, vol. I, pp. 73–94.

Faccenna, C., Becker, T.W., Jolivet, L., Keskin, M., 2013. Mantle convection in the middle East: reconciling Afar upwelling, Arabia indentation and Aegean trench rollback. Earth Planet. Sci. Lett. 375, 254–269.

Faccenna, C., Bellier, O., Martinod, J., Piromallo, C., Regard, V., 2006. Slab detachment beneath eastern Anatolia: a possible cause for the formation of the North Anatolian Fault. Earth Planet. Sci. Lett. 242, 85–97.

Faccenna, C., Jolivet, L., Piromallo, C., Morelli, A., 2003. Subduction and the depth of convection of the Mediterranean mantle. J. Geophys. Res. 108 (B2), 2099. http://dx.doi.org/10.1029/2001JB001690.

Gans, C.R., Beck, S.L., Zandt, G., Biryol, C.B., Ozacar, A.A., 2009. Detecting the limit of slab break-off in central Turkey: new high-resolution Pn tomography results. Geophys. J. Int. 179, 1566–1577.

Genç, S.C., Altunkaynak, S., Karacık, Z., Yılmaz, Y., 2001. The Çubukludağ Graben, Karaburun peninsula: it's tectonic significance in the Neogene geological evolution of the western Anatolia. Geodin. Acta 14, 45–55.

Gessner, K., Gallardo, L.A., Markwitz, V., Ring, U., Thomson, S.N., 2013. What caused the denudation of the Menderes Massif: review of crustal evolution, lithosphere structure, and dynamic topography in southwest Turkey. Gondwana Res. 24, 243–274.

Govers, R., Wortel, M.J.R., 2005. Lithosphere tearing at STEP faults: response to edges of subduction zones. Earth Planet. Sci. Lett. 236, 505–523. http://dx.doi.org/10.1016/j.epsl.2005.03.022.

Gülyüz, E., Kaymakci, N., Meijers, M.J.M., van Hinsbergen, D.J.J., Lefebvre, C., Vissers, R.L.M., Hendriks, B.W.H., Peynircioğlu, A.A., 2013. Late Eocene evolution of the Çiçekdağı Basin (central Turkey): syn-sedimentary compression during microcontinent–continent collision in central Anatolia. Tectonophysics 602, 286–299. http://dx.doi.org/10.1016/j.tecto.2012.07.003.

Gürsoy, H., Piper, J.D.A., Tatar, O., Temiz, H., 1997. A palaeomagnetic study of the Sivas Basin, Central Turkey: crustal deformation during lateral extrusion of the Anatolian Block. Tectonophysics 271, 89–105.

Gürsoy, H., Piper, J.D.A., Tatar, O., 1999. Palaeomagnetic study of the Galatean Volcanic Province, north-central Turkey: neogene deformation at the northern border of the Anatolian Block. Geol. J. 34, 7–23.

Gürsoy, H., Piper, J.D.A., Tatar, O., 2003. Neotectonic deformation in the western sector of tectonic escape in Anatolia: palaeomagnetic study of the Afyon region, central Turkey. Tectonophysics 374, 57–79. http://dx.doi.org/10.1016/S0040-1951(03)00346-9.

Gürsoy, H., Tatar, O., Piper, J.D.A., Heimann, A., Kochulut, F., Mesci, B.L., 2009. Palaeomagnetic study of Tertiary volcanic domains in Southern Turkey and Neogene anticlockwise rotation of the Arabian Plate. Tectonophysics 465, 114–127.

Hetzel, R., Ring, U., Akal, C., Troesch, M., 1995. Miocene NNE-directed extensional unroofing in the Menderes Massif, southwestern Turkey. J. Geol. Soc. Lond. 152, 639–654.

Hetzel, R., Zwingmann, H., Mulch, A., Gessner, K., Akal, C., Hampel, A., Güngör, T., Petschick, R., Mikes, T., Wedin, F., 2013. Spatio-temporal evolution of brittle normal faulting and fluid infiltration in detachment fault systems—a case study from the Menderes Massif, western Turkey. Tectonics 32 (3), 364–376.

Horner, F., Freeman, R., 1982. Preliminary palaeomagnetic results from the Ionian Zone, western Greece. Eos 63 (51), 1273.

Horner, F., Freeman, R., 1983. Palaeomagnetic evidence from Pelagic Limestones for clockwise rotation of the Ionian zone, western Greece. Tectonophysics 98, 11–27. http://dx.doi.org/10.1016/0040-1951(83)90208-1.

Hrouda, F., 1982. Magnetic anisotropy of rocks and its application in geology and geophysics. Geophys. Surv. 5, 37–82.

Jelinek, V., 1978. Statistical processing of anisotropy of magnetic susceptibility on groups of specimens. Stud. Geophys. Geod. 22, 50–62.

Jelinek, V., 1981. Characterisation of the magnetic fabrics of rocks. Tectonophysics 79 (3–4), T63–T67.

Jolivet, L., Lecomte, E., Huet, B., Denèle, Y., Lacombe, O., Labrousse, L., Le Pourhiet, L., Mehl, C., 2010. The North Cycladic detachment system. Earth Planet. Sci. Lett. 289, 87–104. http://dx.doi.org/10.1016/j.epsl.2009.10.032.

Jolivet, L., Faccenna, C., Huet, B., Labrousse, L., Le Pourhiet, L., Lacombe, O., Lacomte, E., Burov, E., Denele, Y., Brun, J., Philippon, M., Paul, A., Salaun, B., Karabulut, H., Piromallo, C., Monie, P., Gueydan, F., Okay, A., Oberhänsli, R., Pourteau, A., Augier, R., Gadenne, L., Driussi, O., 2013. Aegean tectonics: strain localization, slab tearing and trench retreat. Tectonophysics 597–598, 1–33.

Kahle, H.-G., Concord, M., Peter, Y., Geiger, A., Reilinger, R., Barka, A., Veis, G., 2000. GPS derived strain rate field within the boundary zones of the Eurasian, African, and Arabian plates. J. Geophys. Res. 105, 23,353–23,370.

Kaya, O., 1981. Miocene reference section for the coastal parts of West Anatolia. Newsl. Stratigr. 10, 164–191.

Kaymakci, N., 2006. Kinematic development and paleostress analysis of Denizli Basin (W Turkey): implications of spatial variation of relative paleostress magnitudes and orientations. J. Asian Earth Sci. 27, 207–222.

Kaymakci, N., Aldanmaz, E., Langereis, C., Spell, T.L., Gurer, O.F., Zanetti, K.A., 2007. Late Miocene transcurrent tectonics in NW Turkey: evidence from palaeomagnetism and ^{40}Ar–^{39}Ar dating of alkaline volcanic rocks. Geol. Mag. 144 (2), 379–392.

Kirschvink, J.L., 1980. The least-squares line and plane and the analysis of palaeomagnetic data. Geophys. J. R. Astron. Soc. 62, 699–718.

Kissel, C., Poisson, A., 1986. Étude paléomagnetique des formations néogènes du bassin d'Antalya (Taurides occidentales-Turquie). C. R. Acad. Sci. Ser. II 302 (10), 711–716.

Kissel, C., Poisson, A., 1987. Étude paléomagnetique préliminaire des formations cénozoïques des Bey Daglari (Taurides occidentales, Turquie). C. R. Acad. Sci. Ser. II 304 (8), 343–348.

Kissel, C., Laj, C., 1988. The tertiary geodynamical evolution of the Aegean arc: a paleomagnetic reconstruction. Tectonophysics 146, 183–201. http://dx.doi.org/10.1016/0040-1951(88)90090-X.

Kissel, C., Jamet, M., Laj, C., 1984. Paleomagnetic evidence of Miocene and Pliocene rotational deformations of the Aegean area. In: Dixon, J.E., Robertson, A.H.F. (Eds.), The Geological Evolution of the Eastern Mediterranean. In: Geological Soc. Spec. Publ., vol. 17, pp. 669–679.

Kissel, C., Laj, C., Müller, C., 1985. Tertiary geodynamical evolution of northwestern Greece: paleomagnetic results. Earth Planet. Sci. Lett. 72, 190–204. http://dx.doi.org/10.1016/0012-821X(85)90005-6.

Kissel, C., Laj, C., Şengör, A.M.C., Poisson, A., 1987. Paleomagnetic evidence for rotation in opposite senses of adjacent blocks in northeastern Aegea and Western Anatolia. Geophys. Res. Lett. 14 (9), 907–910.

Kissel, C., Laj, C., Poisson, A., Simeakis, K., 1989. A pattern of block rotations in central Aegean. In: Kissel, C., Laj, C. (Eds.), Paleomagnetic Rotations and Continental Deformation. In: NATO ASI Ser., Ser. C, vol. 254. Kluwer Acad., Dordrecht, Netherlands, pp. 115–129.

Kissel, C., Averbuch, O., de Lamotte, D.F., Monod, O., Allerton, S., 1993. First paleomagnetic evidence for a post-Eocene clockwise rotation of the western Taurides thrust belt east of the Isparta reentrant (southwestern Turkey). Earth Planet. Sci. Lett. 117 (1–2), 1–14. http://dx.doi.org/10.1016/0012-821X(93)90113-N.

Koç, A., Kaymakci, N., 2013. Kinematics of Sürgü fault zone (Malatya, Turkey): a remote sensing study. J. Geodyn. 65, 292–307.

Koçyiğit, A., Yusufoğlu, H., Bozkurt, E., 1999. Evidence from the Gediz Graben for episodic two-stage extension in western Turkey. J. Geol. Soc. Lond. 156, 605–616.

Kondopoulou, D., Şen, Ş., Aidona, E., van Hinsbergen, D.J.J., Koufos, G., 2011. Rotation history of Chios Island, Greece since the Middle Miocene. J. Geodyn. 51, 327–338.

Krijgsman, W., Duermeijer, C.E., Langereis, C.G., De Bruijn, H., Saraç, G., Andriessen, P.A.M., 1996. Magnetic polarity stratigraphy of late Oligocene to middle Miocene

mammal-bearing continental deposits in Central Anatolia (Turkey). Newsl. Stratigr. 34, 13–29.
Laj, C., Jamet, M., Sorel, D., Valente, J.P., 1982. First paleomagnetic results from Mio-Pliocene series of the Hellenic Sedimentary arc. Tectonophysics 86, 45–67. http://dx.doi.org/10.1016/0040-1951(82)90061-0.
Le Pichon, X., Angelier, J., 1979. The Hellenic arc and trench system: a key to the neotectonic evolution of the eastern Mediterranean area. Tectonophysics 60, 1–42.
Le Pichon, X., Chamot-Rooke, N., Lallemant, S., Noomen, R., Veis, G., 1995. Geodetic determination of the kinematics of central Greece with respect to Europe: implications for eastern Mediterranean tectonics. J. Geophys. Res. 100, 12675–12690.
Lips, A.L.W., Cassard, D., Sözbilir, H., Yılmaz, H., Wijbrans, J.R., 2001. Multistage exhumation of the Menderes Massif, western Anatolia (Turkey). Int. J. Earth Sci. 89, 781–792.
Márton, E., Papanikolaou, D.J., Lekkas, E., 1990. Paleomagnetic results from the Pindos, Paxos and Ionian zones of Greece. Phys. Earth Planet. Inter. 62, 60–69. http://dx.doi.org/10.1016/0031-9201(90)90192-Z.
Mauritsch, H.J., Scholger, R., Bushati, S.L., Ramiz, H., 1995. Palaeomagnetic results from southern Albania and their significance for the geodynamic evolution of the Dinarides, Albanides and Hellenides. Tectonophysics 242, 5–18. http://dx.doi.org/10.1016/0040-1951(94)00150-8.
Mauritsch, H.J., Scholger, R., Bushati, S.L., Xhomo, A., 1996. Palaeomagnetic investigations in northern Albania and their significance for the geodynamic evolution of the Adriatic–Aegean realm. In: Morris, A., Tarling, D.H. (Eds.), Palaeomagnetism and Tectonics of the Mediterranean Region. In: Geol. Soc. Spec. Publ., vol. 105, pp. 265–275.
McFadden, P.L., McElhinny, M.W., 1988. The combined analysis of remagnetisation circles and direct observations in paleomagnetism. Earth Planet. Sci. Lett. 87, 161–172.
McFadden, P.L., McElhinny, M.W., 1990. Classification of the reversal test in palaeomagnetism. Geophys. J. Int. 103, 725–729.
Meulenkamp, J.E., Wortel, M.J.R., van Wamel, W.A., Spakman, W., Hoogerduyn Strating, E., 1988. On the Hellenic subduction zone and the geodynamical evolution of Crete since the late middle Miocene. Tectonophysics 146, 203–215.
Morris, A., 1995. Rotational deformation during Palaeogene thrusting and basin closure in eastern central Greece: palaeomagnetic evidence from Mesozoic carbonates. Geophys. J. Int. 121, 827–847. http://dx.doi.org/10.1111/j.1365-246X.1995.tb06442.x.
Morris, A., Robertson, A.H.F., 1993. Miocene remagnetisation of carbonate platform and Antalya Complex units within the Isparta Angle, SW Turkey. Tectonophysics 220, 243–266. http://dx.doi.org/10.1016/0040-1951(93)90234-B.
Morris, A., Anderson, M., 1996. First palaeomagnetic results from the Cycladic Massif, Greece, and their implications for Miocene extension directions and tectonic models in the Aegean. Earth Planet. Sci. Lett. 142, 397–408.
Mullender, T.A.T., van Velzen, A.J., Dekkers, M.J., 1993. Continuous drift correction and separate identification of ferrimagnetic and paramagnetic contribution in thermomagnetic runs. Geophys. J. Int. 114, 663–672.
Naylor, M.A., Mandl, G., Sijpesteijn, C.H.K., 1986. Fault geometries in basement-induced wrench faulting under different initial stress states. J. Struct. Geol. 8, 737–752.
Okay, A.İ., 2001. Stratigraphic and metamorphic inversions in the central Menderes Massif: a new structural model. Int. J. Earth Sci. 89, 709–727.
Orbay, N., Sanver, M., Hisarli, T., Isseven, T., Ozcep, F., 2000. Karaburun Yarımadasının paleomagnetizması ve tektonik evrimi [Paleomagnetism and tectonic evolution of Karaburun Peninsula]. In: Batı Anadolu' nun Depremselliği Sempozyumu Kitabi, pp. 59–67 (in Turkish).
Özkaymak, Ç., Sözbilir, H., 2008. Stratigraphic and structural evidence for fault reactivation: the active Manisa fault zone, western Anatolia. Turk. J. Earth Sci. 17 (3), 615–635.
Özkaymak, Ç., Sözbilir, H., Uzel, B., 2013. Neogene-Quaternary evolution of the Manisa Basin: evidence for variation in the stress pattern of the İzmir-Balıkesir transfer zone, Western Anatolia. J. Geodyn. 65, 117–135. http://dx.doi.org/10.1016/j.jog.2012.06.004.
Paula, A., Karabulut, H., Mutlu, A.K., Salaün, G., 2014. A comprehensive and densely sampled map of shear-wave azimuthal anisotropy in the Aegean–Anatolia region. Earth Planet. Sci. Lett. 389, 14–22.
Pe-Piper, G., Piper, D.J.W., Matarangas, D., 2002. Regional implications of geochemistry and style of emplacement of Miocene I-type diorite and granite, Delos, Cyclades, Greece. Lithos 60, 47–66.
Philippon, M., Brun, J.P., Gueydan, F., 2012. Deciphering subduction from exhumation in the segmented Cycladic Blueschist Unit (Central Aegean, Greece). Tectonophysics 524–525, 116–134.
Piper, J.D.A., Gürsoy, H., Tatar, O., Beck, M.E., Rao, A., Koçbulut, F., Mesci, B.L., 2010. Distributed neotectonic deformation in the Anatolides of Turkey: a palaeomagnetic analysis. Tectonophysics 488, 31–50.
Platzman, E.S., Tapirdamaz, C., Sanver, M., 1998. Neogene anticlockwise rotation of Anatolia (Turkey): preliminary palaeomagnetic and geochronological results. Tectonophysics 299, 175–189. http://dx.doi.org/10.1016/S0040-1951(98)00204-2.
Reinecker, J., Heidbach, O., Tingay, M., Sperner, B., Müller, B., 2005. The release 2005 of the World Stress Map. Available online at www.world-stress-map.org.
Ring, U., Glodny, J., Will, T., Thomson, S., 2010. The Hellenic subduction system: high-pressure metamorphism, exhumation, normal faulting, and large-scale extension. Earth Planet. Sci. 38, 45–76. http://dx.doi.org/10.1146/annurev.earth.050708.170910.
Ring, U., Johnson, C., Hetzel, R., Gessner, K., 2003. Tectonic denudation of a Late Cretaceous–Tertiary collisional belt: regionally symmetric cooling patterns and their relation to extensional faults in the Anatolide belt of western Turkey. Geol. Mag. 140 (4), 421–441. http://dx.doi.org/10.1017/S0016756803007878.
Ring, U., Susanne, L., Matthias, B., 1999. Structural analysis of a complex nappe sequence and late orogenic basins from the Aegean Island of Samos, Greece. J. Struct. Geol. 21, 1575–1601.
Scheepers, P., 1992. No tectonic rotation for the Apulia–Gargano foreland in the Pleistocene. Geophys. Res. Lett. 19 (22), 2275–2278. http://dx.doi.org/10.1029/92GL02440.
Şen, S., Seyitoğlu, G., 2009. Magnetostratigraphy of early–middle Miocene deposits from east–west trending Alaşehir and Büyük Menderes grabens in western Turkey, and its tectonic implications. In: van Hinsbergen, D.J.J., et al. (Eds.), Collision and Collapse at the Africa–Arabia–Eurasia Subduction Zone. In: Geol. Soc. (Lond.) Spec. Publ., vol. 311, pp. 321–342.
Şengör, A.M.C., Görür, N., Şaroğlu, F., 1985. Strike-slip faulting and related basin formation in zones of tectonic escape: Turkey as a case study. In: Biddle, K., Christie-Blick, N. (Eds.), Strike-Slip Deformation, Basin Formation and Sedimentation. In: Society of Economic Paleontologists and Mineralogists, Special Publications, vol. 37, pp. 227–264.
Seyitoğlu, G., Scott, B.C., 1992. The age of the Büyük Menderes graben (west Turkey) and its tectonic implications. Geol. Mag. 129, 239–242.
Seyitoğlu, G., Scott, B.C., Rundle, C.C., 1992. Timing of Cenozoic extensional tectonics in west Turkey. J. Geol. Soc. 149, 533–538. http://dx.doi.org/10.1144/gsjgs.149.4.0533.
Sözbilir, H., 2001. Extensional tectonics and the geometry of related macroscopic structures: field evidence from the Gediz detachment, western Turkey. Turk. J. Earth Sci. 10, 51–67.
Sözbilir, H., 2002. Geometry and origin of folding in the Neogene sediments of the Gediz Graben, Western Anatolia, Turkey. Geodin. Acta 15, 277–288.
Sözbilir, H., Emre, T., 1990. Neogene stratigraphy and structure of the northern rim of the Büyük Menderes graben. In: Savaşçın, M.Y., Eronat, A.H. (Eds.), Proceedings of International Earth Science Colloquium on the Aegean Region 2, pp. 314–322.
Sözbilir, H., Emre, T., 1996. Supradetachment basin and rift basin developed during the neotectonic evolution of the Menderes Massif. In: Geological Congress of Turkey, Ankara, Abstracts, pp. 300–301.
Sözbilir, H., İnci, U., Erkül, F., Sümer, Ö., 2003. An active intermittent transfer zone accommodating N–S extension in western Anatolia and its relation to the North Anatolian fault system. In: International Workshop on the North Anatolian, East Anatolian and Dead Sea Fault Systems: Recent Progress in Tectonics and Palaeoseismology and Field Training Course in Palaeoseismology, Ankara, Abstracts, p. 87.
Sözbilir, H., Sarı, B., Uzel, B., Sümer, Ö., Akkiraz, S., 2011. Tectonic implications of transtensional supradetachment basin development in an extension-parallel transfer zone: the Kocaçay Basin, western Anatolia, Turkey. Basin Res. 23, 423–448. http://dx.doi.org/10.1111/j.1365-2117.2010.00496.x.
Speranza, F., Kissel, C., 1993. First paleomagnetism of Eocene rocks from Gargano: widespread overprint or non-rotation? Geophys. Res. Lett. 20 (23), 2627–2630. http://dx.doi.org/10.1029/93GL02816.
Speranza, F., Kissel, C., Islami, I., Hyseni, A., Laj, C., 1992. First paleomagnetic evidence for rotation of the Ionian zone of Albania. Geophys. Res. Lett. 19 (7), 697–700. http://dx.doi.org/10.1029/92GL00575.
Speranza, F., Islami, I., Kissel, C., Hyseni, A., 1995. Palaeomagnetic evidence for Cenozoic clockwise rotation of the external Albanides. Earth Planet. Sci. Lett. 129, 121–134. http://dx.doi.org/10.1016/0012-821X(94)00231-M.
Tauxe, L., Kent, D.V., 2004. A simplified statistical model for the geomagnetic field and the detection of shallow bias in paleomagnetic inclinations: was the ancient magnetic field dipolar? In: Channell, J.E.T., et al. (Eds.), Time-Scales of the Paleomagnetic Field. In: Geophysical Monograph Series, vol. 145, pp. 101–115.
Taylor, M., Yin, A., Ryerson, F.J., Kapp, P., Ding, L., 2003. Conjugate strike–slip faulting along the Bangong–Nujiang suture zone accommodates coeval east–west extension and north–south shortening in the interior of the Tibetan Plateau. Tectonics 22 (4), 1801–1821. http://dx.doi.org/10.1029/2002TC001361.
Uzel, B., Sözbilir, H., 2008. A first record of strike-slip basin in western Anatolia and its tectonic implication: the Cumaovası basin as an example. Turk. J. Earth Sci. 17, 559–591.
Uzel, B., Sözbilir, H., Özkaymak, Ç., 2012. Neotectonic evolution of an actively growing superimposed basin in western Anatolia: the inner bay of İzmir, Turkey. Turk. J. Earth Sci. 22 (4), 439–471. http://dx.doi.org/10.3906/yer-0910-11.
Uzel, B., Sözbilir, H., Özkaymak, Ç., Kaymakcı, N., Langereis, C.G., 2013. Structural evidence for strike-slip deformation in the İzmir–Balıkesir transfer zone and consequences for late Cenozoic evolution of western Anatolia (Turkey). J. Geodyn. 65, 94–116.
Uzel, B., Kuiper, K., Sözbilir, H., Kaymakcı, N., Langereis, C.G., Özkaymak, Ç., Özkaptan, M., in preparation. Geochronological evidence for a short time break on the

İzmir-Balıkesir Transfer Zone located between Aegean & West Anatolian extensional provinces, Turkey.

Uzel, B., Sümer, Ö., Sözbilir, H., Kaymakcı, N., Langereis, C.G., Kuiper, K., Özkaymak, Ç., İnci, U., in preparation. Paleomagnetic and geochronologic evidence for an unconformity during the Middle Miocene Climatic Optimum (MMCO): implications for exhumation of Menderes metamorphic core complex and related basin formation – continuous or episodic?

van Hinsbergen, D.J.J., Langereis, C.G., Meulenkamp, J.E., 2005a. Revision of the timing, magnitude and distribution of Neogene rotations in the western Aegean region. Tectonophysics 396, 1–34.

van Hinsbergen, D.J.J., Hafkenscheid, E., Spakman, W., Meulenkamp, J.E., Wortel, R., 2005b. Nappe stacking resulting from subduction of oceanic and continental lithosphere below Greece. Geology 33, 325–328.

van Hinsbergen, D.J.J., Krijgsman, W., Langereis, C.G., Cornée, J.J., Duermeijer, C.E., van Vugt, N., 2007. Discrete Plio-Pleistocene phases of tilting and counterclockwise rotation in the southeastern Aegean arc (Rhodos, Greece): early Pliocene formation of the south Aegean left-lateral strike-slip system. J. Geol. Soc. 164, 1133–1144. http://dx.doi.org/10.1144/0016-76492006-061.

van Hinsbergen, D.J.J., Dupont-Nivet, G., Nakov, R., Oud, K., Panaiotu, C., 2008. No significant post-Eocene rotation of the Moesian Platform and Rhodope (Bulgaria): implications for the kinematic evolution of the Carpathian and Aegean arcs. Earth Planet. Sci. Lett. 273, 345–358. http://dx.doi.org/10.1016/j.epsl.2008.06.051.

van Hinsbergen, D.J.J., Kaymakci, N., Spakman, W., Torsvik, T.H., Amaru, M., 2010. Reconciling geological history with mantle structure in western Turkey. Earth Planet. Sci. Lett. 297, 674–686.

van Hinsbergen, D.J.J., Dekkers, M.J., Bozkurt, E., Koopman, M., 2010a. Exhumation with a twist: paleomagnetic constraints on the evolution of the Menderes metamorphic core complex, western Turkey. Tectonics 29 (3), TC3009. http://dx.doi.org/10.1029/2009TC002596.

van Hinsbergen, D.J.J., Dekkers, M.J., Koç, A., 2010b. Testing Miocene remagnetization of Bey Dağları: timing and amount of Neogene rotations in SW Turkey. Turk. J. Earth Sci. 19, 123–156. http://dx.doi.org/10.3906/yer-0904-1.

van Hinsbergen, D.J.J., 2010c. A key extensional metamorphic core complex reviewed and restored: the Menderes Massif of western Turkey. Earth-Sci. Rev. 102, 60–76.

van Hinsbergen, D.J.J., Mensink, M., Langereis, C.G., Maffione, M., Spalluto, L., Tropeano, M., Sabato, L., 2014. Did Adria rotate relative to Africa? Solid Earth Discus. 6, 937–983. http://dx.doi.org/10.5194/sed-6-937-2014.

Vasiliev, I., Franke, C., Meeldijk, J.D., Dekkers, M.J., Langereis, C.G., Krijgsman, W., 2008. Putative greigite magnetofossils from the Pliocene epoch. Nat. Geosci. 1 (11), 782–786.

Walcott, C.R., White, S.H., 1998. Constraints on the kinematics of post-orogenic extension imposed by stretching lineations in the Aegean region. Tectonophysics 298, 155–175.

Watson, G.S., 1983. Large sample theory of the Langevin distribution. J. Stat. Plan. Infer. 8, 245–256.

Wortel, M.J.R., Spakman, W., 2000. Subduction and slab detachment in the Mediterranean–Carpathian region. Science 290, 1910–1917.

Yin, A., 2010. Cenozoic tectonic evolution of Asia: a preliminary synthesis. Tectonophysics 488, 293–325.

Yin, A., Taylor, M.H., 2011. Mechanics of V-shaped conjugate strike-slip faults and the corresponding continuum mode of continental deformation. Geol. Soc. Am. Bull. 123, 1798–1821. http://dx.doi.org/10.1130/B30159.1.

Zijderveld, J.D.A., 1967. A.C. demagnetization of rocks: analysis of results. In: Collinson, D.W., Creer, K.M., Runcorn, S.K. (Eds.), Methods in Palaeomagnetism. Elsevier, Amsterdam, pp. 254–286.